Fermion and scalar phenomenology of a two-Higgs-doublet model with S_3

A. E. Cárcamo Hernández,[1,*] I. de Medeiros Varzielas,[2,†] and E. Schumacher[3,‡]

[1]*Universidad Técnica Federico Santa María and Centro Científico-Tecnológico de Valparaíso Casilla 110-V, Valparaíso, Chile*

[2]*School of Physics and Astronomy, University of Southampton, Southampton SO17 1BJ, United Kingdom*

[3]*Fakultät für Physik, Technische Universität Dortmund D-44221 Dortmund, Germany*

(Received 8 September 2015; published 11 January 2016)

We propose a two-Higgs-doublet model where the symmetry is extended by $S_3 \otimes Z_3 \otimes Z'_3 \otimes Z_{14}$ and the field content is enlarged by extra $SU(2)_L$ singlet scalar fields. S_3 makes the model predictive and leads to viable fermion masses and mixing. The observed hierarchy of the quark masses arises from the Z'_3 and Z_{14} symmetries. The light neutrino masses are generated through a type I seesaw mechanism with two heavy Majorana neutrinos. In the lepton sector we obtain mixing angles that are nearly tri-bimaximal, in excellent agreement with the observed lepton parameters. The vacuum expectation values required for the model are naturally obtained from the scalar potential, and we analyze the scalar sector properties to further constrain the model through rare top decays (like $t \to ch$), the $h \to \gamma\gamma$ decay channel and the T and S parameters.

DOI: 10.1103/PhysRevD.93.016003

I. INTRODUCTION

The flavor puzzle is not understood in the context of the Standard Model (SM), which does not specify the Yukawa structures and has no justification for the number of generations. As such, extensions addressing the fermion masses and mixing are particularly appealing. With neutrino experiments increasingly constraining the mixing angles in the leptonic sector many models focus only on this sector, aiming to explain the near tri-bimaximal structure of the Pontercorvo-Maki-Nakagawa-Sakata (PMNS) matrix through some non-Abelian symmetry.

Discrete flavor symmetries have shown a lot of promise and S_3, as the smallest non-Abelian group, has been extensively studied in the literature since [1], with interesting results for quarks, leptons or both, and remains a popular group [2–15]. Other popular groups are the smallest groups with triplet representations, particularly A_4 which has only a triplet and three distinct singlets. A_4 was used in [16–20] and more recently in [21–35]. With just triplets and singlet representations the groups T_7 [36–43] and $\Delta(27)$ [44–52] are also promising as flavor symmetries. For recent reviews on the use of discrete flavor groups, see Refs. [53,54].

In this work we make use of the S_3 group to formulate a two-Higgs-doublet model (2HDM) with an extra $S_3 \otimes Z_3 \otimes Z'_3 \otimes Z_{14}$ symmetry. Assigning the SM fermions under this symmetry and using scalars transforming under the different irreducible representations of S_3, we provide an existence proof of models leading to the viable mixing inspired quark textures presented in [55], by building a minimal realization. We then consider the model in the lepton sector where we obtain viable masses and mixing angles by using assignments that lead to a charged lepton texture similar to that of the down-type quarks, with the neutrino sector being completed through a type I seesaw. We discuss the scalar potential in some detail, showing that it leads to the vacuum expectation values (VEVs) used to obtain the fermion masses, and analyzing phenomenological processes that constrain the parameters of the model such as $t \to ch$ and $h \to \gamma\gamma$.

The paper is outlined as follows. In Sec. II we describe the field and symmetry content of the model, including a brief revision of the quark mass and mixing angles presented in [55] (Sec. II A) and the equivalent analysis for the lepton sector (Sec. II B). Section III contains the analysis of the phenomenology associated with the extended scalar sector, presenting the Yukawa couplings and an analysis of rare top decays, and then considering the $h \to \gamma\gamma$ rate (Sec. III A) and the T and S parameters (Sec. III B). We present our conclusions in Sec. IV. We relegate some technical discussions that are relevant for the paper to the Appendix.

II. THE MODEL

We consider an extension of the SM with extra scalar fields and discrete symmetries, which reproduces the predictive mixing inspired textures proposed in Ref. [55]; i.e. the Cabibbo mixing arises from the down-type quark sector whereas the up-type quark sector contributes to the remaining mixing angles. These textures describe the charged fermion masses and quark mixing pattern in terms of different powers of the Wolfenstein

*antonio.carcamo@usm.cl
†ivo.de@soton.ac.uk
‡erik.schumacher@tu-dortmund.de

parameter $\lambda = 0.225$ and order one parameters. Because of the required mismatch between the down-type quark and up-type quark textures, to obtain these textures in a model we use two-Higgs doublets distinguished by a symmetry (in our model, a Z_3). In the following, we describe our 2HDM with the inclusion of the $S_3 \otimes Z_3 \otimes Z_3' \otimes Z_{14}$ discrete symmetry and four singlet scalar fields, assigned in an S_3 doublet, one S_3 trivial singlet and one S_3 nontrivial singlet. We use the S_3 discrete group since it is the smallest non-Abelian group, having a doublet and two singlets as irreducible representations. The full symmetry $\mathcal{G}$ of the model is broken spontaneously in two steps:

$$\begin{gathered} \mathcal{G} = SU(3)_C \otimes SU(2)_L \otimes U(1)_Y \otimes S_3 \otimes Z_3 \otimes Z_3' \otimes Z_{14} \\ \Downarrow \Lambda \\ SU(3)_C \otimes SU(2)_L \otimes U(1)_Y \otimes Z_3 \\ \Downarrow \Lambda_{\mathrm{EW}} \\ SU(3)_C \otimes U(1)_{em}, \end{gathered} \tag{1}$$

where the different symmetry breaking scales satisfy the hierarchy $\Lambda \gg \Lambda_{\mathrm{EW}}$, where $\Lambda_{\mathrm{EW}} = 246$ GeV is the electroweak symmetry breaking scale.

The content of the model, which includes the particle assignments under the different symmetries, is shown in Tables I and II. The S_3 symmetry reduces the number of parameters in the Yukawa sector of this 2HDM, making it more predictive. The Z_3 symmetry allows us to completely decouple the bottom quark from the remaining down and strange quarks. As can be seen from the scalar field assignments, the two scalar $SU(2)_L$ doublets have different Z_3 charges (ϕ_1 being neutral). The Z_3' and Z_{14} symmetries shape the hierarchical structure of the quark mass matrices necessary to get a realistic pattern of quark masses and mixing.

The Higgs doublets ϕ_l ($l = 1,\ 2$) acquire VEVs that break $SU(2)_L$:

$$\phi_l = \begin{pmatrix} 0 \\ \frac{v_l}{\sqrt{2}} \end{pmatrix}, \qquad l = 1, 2. \tag{2}$$

We decompose the Higgs fields around this minimum as

$$\phi_l = \begin{pmatrix} \varphi_l^+ \\ \frac{1}{\sqrt{2}}(v_l + \rho_l + i\eta_l) \end{pmatrix} = \begin{pmatrix} \frac{1}{\sqrt{2}}(\omega_l + i\tau_l) \\ \frac{1}{\sqrt{2}}(v_l + \rho_l + i\eta_l) \end{pmatrix}, \tag{3}$$

where

$$\langle \rho_l \rangle = \langle \eta_l \rangle = \langle \omega_l \rangle = \langle \tau_l \rangle = 0, \qquad l = 1, 2. \tag{4}$$

From an analysis of the scalar potential (see Appendix B), we obtain the following VEVs for the SM singlet scalars:

$$\langle \xi \rangle = v_\xi (1, 0), \qquad \langle \chi \rangle = v_\chi, \qquad \langle \zeta \rangle = v_\zeta; \tag{5}$$

i.e., the VEV of ξ is aligned as (1,0) in the S_3 direction.

For the up- and down-type quarks, the Yukawa terms invariant under the symmetries are

$$\begin{aligned} \mathcal{L}_Y^U = {} & \varepsilon_{33}^{(u)} \bar{q}_{3L} \tilde{\phi}_1 u_{3R} + \varepsilon_{23}^{(u)} \bar{q}_{2L} \tilde{\phi}_2 u_{3R} \frac{\chi^2}{\Lambda^2} \\ & + \varepsilon_{13}^{(u)} \bar{q}_{1L} \tilde{\phi}_2 u_{3R} \frac{\chi^3}{\Lambda^3} + \varepsilon_{22}^{(u)} \bar{q}_{2L} \tilde{\phi}_1 U_R \frac{\xi \chi^3}{\Lambda^4} \\ & + \varepsilon_{11}^{(u)} \bar{q}_{1L} \tilde{\phi}_1 U_R \frac{\xi \chi^4 \zeta^3}{\Lambda^8} + \mathrm{H.c.} \end{aligned} \tag{6}$$

$$\begin{aligned} \mathcal{L}_Y^D = {} & \varepsilon_{33}^{(d)} \bar{q}_{3L} \phi_1 d_{3R} \frac{\chi^3}{\Lambda^3} + \varepsilon_{22}^{(d)} \bar{q}_{2L} \phi_2 d_{2R} \frac{\chi^5}{\Lambda^5} \\ & + \varepsilon_{12}^{(d)} \bar{q}_{1L} \phi_2 d_{2R} \frac{\chi^6}{\Lambda^6} + \varepsilon_{21}^{(d)} \bar{q}_{2L} \phi_2 d_{1R} \frac{\chi^6}{\Lambda^6} \\ & + \varepsilon_{11}^{(d)} \bar{q}_{1L} \phi_2 d_{1R} \frac{\chi^7}{\Lambda^7} + \mathrm{H.c.} \end{aligned} \tag{7}$$

The invariant Yukawa terms for charged leptons and neutrinos are

$$\begin{aligned} \mathcal{L}_Y^l = {} & \varepsilon_{33}^{(l)} \bar{l}_{3L} \phi_1 l_{3R} \frac{\chi^3}{\Lambda^3} + \varepsilon_{23}^{(l)} \bar{l}_{2L} \phi_1 l_{3R} \frac{\chi^3}{\Lambda^3} \\ & + \varepsilon_{22}^{(l)} \bar{l}_{2L} \phi_1 l_{2R} \frac{\chi^5}{\Lambda^5} + \varepsilon_{32}^{(l)} \bar{l}_{3L} \phi_1 l_{2R} \frac{\chi^5}{\Lambda^5} \\ & + \varepsilon_{11}^{(l)} \bar{l}_{1L} \phi_2 l_{1R} \frac{\chi^7 \zeta}{\Lambda^8} + \mathrm{H.c.} \end{aligned} \tag{8}$$

$$\begin{aligned} \mathcal{L}_Y^\nu = {} & \varepsilon_{11}^{(\nu)} \bar{l}_{1L} \tilde{\phi}_2 \nu_{1R} \frac{\chi^3}{\Lambda^3} + \varepsilon_{12}^{(\nu)} \bar{l}_{1L} \tilde{\phi}_2 \nu_{2R} \frac{\chi^3}{\Lambda^3} + \varepsilon_{21}^{(\nu)} \bar{l}_{2L} \tilde{\phi}_1 \nu_{1R} \\ & + \varepsilon_{22}^{(\nu)} \bar{l}_{2L} \tilde{\phi}_1 \nu_{2R} + \varepsilon_{31}^{(\nu)} \bar{l}_{3L} \tilde{\phi}_1 \nu_{1R} + \varepsilon_{32}^{(\nu)} \bar{l}_{3L} \tilde{\phi}_1 \nu_{2R} \\ & + M_1 \bar{\nu}_{1R} \nu_{1R}^c + M_2 \bar{\nu}_{2R} \nu_{2R}^c + M_{12} \bar{\nu}_{1R} \nu_{2R}^c + \mathrm{H.c.} \end{aligned} \tag{9}$$

TABLE I. Assignments of the SM fermions under the flavor symmetries.

Field	q_{1L}	q_{2L}	q_{3L}	U_R	u_{3R}	d_{1R}	d_{2R}	d_{3R}	l_{1L}	l_{2L}	l_{3L}	l_{1R}	l_{2R}	l_{3R}	ν_{1R}	ν_{2R}
S_3	1	1	1	2	1	1	1	1	1	1	1	1'	1	1	1	1
Z_3	0	0	1	0	1	2	2	1	2	0	0	1	0	0	0	0
Z_3'	0	0	0	0	0	0	0	0	0	0	0	2	0	0	0	0
Z_{14}	−3	−2	0	1	0	4	3	3	−3	0	0	4	5	3	0	0

TABLE II. Assignments of the scalars under $SU(2)_L$ and the flavor symmetries.

Field	ϕ_1	ϕ_2	ξ	χ	ζ
$SU(2)_L$	2	2	1	1	1
S_3	1	1	2	1	1’
Z_3	0	1	0	0	0
Z_3'	0	0	0	0	1
Z_{14}	0	0	0	−1	0

The Z_{14} symmetry is the smallest cyclic symmetry that allows $\frac{\chi^7}{\Lambda^7}$ in the Yukawa terms responsible for the down quark and electron masses, which we want to suppress by λ^7 ($\lambda = 0.225$ is one of the Wolfenstein parameters) without requiring small dimensionless Yukawa couplings. Furthermore, the Z_3' symmetry is responsible for coupling the scalar ζ with U_R as well as with l_{1R}, which helps to explain the smallness of the up quark and electron mass in this model. The hierarchy of charged fermion masses and quark mixing matrix elements is therefore explained by both the Z_3' and Z_{14} symmetries. Given that in this scenario the quark masses are related with the quark mixing parameters, we set the VEVs of the $SU(2)_L$ singlet scalars with respect to the Wolfenstein parameter λ and the new physics scale Λ:

$$v_\xi \sim v_\zeta \sim v_\chi = \lambda\Lambda. \tag{10}$$

These scalars therefore acquire VEVs at a scale unrelated to $\Lambda_{\rm EW}$. We have checked numerically that this regime is a valid minimum of the global potential for a suitable region of the parameter space (see Appendix B). As we will see in the following sections, in order to obtain realistic fermion masses and mixing without requiring a strong hierarchy among the Yukawa couplings, the VEVs of the $SU(2)_L$ doublets (v_1 and v_2) should be of the same order of magnitude.

A. Quark masses and mixing

Using Eqs. (6) and (7) we find the mass matrices for up- and down-type quarks in the form

$$M_U = \frac{v}{\sqrt{2}}\begin{pmatrix} c_1\lambda^8 & 0 & a_1\lambda^3 \\ 0 & b_1\lambda^4 & a_2\lambda^2 \\ 0 & 0 & a_3 \end{pmatrix}, \qquad M_D = \frac{v}{\sqrt{2}}\begin{pmatrix} e_1\lambda^7 & f_1\lambda^6 & 0 \\ e_2\lambda^6 & f_2\lambda^5 & 0 \\ 0 & 0 & g_1\lambda^3 \end{pmatrix}, \tag{11}$$

where a_k ($k = 1, 2, 3$), b_1, c_1, g_1, f_1, f_2, e_1 and e_2 are $\mathcal{O}(1)$ parameters. Here we assume that all dimensionless parameters given in Eq. (11) are real except for a_3, which we assume to be complex. These are the viable quark textures presented in [55], which we briefly review here.

The Hermitian combinations $M_U M_U^\dagger$ and $M_D M_D^T$ are

$$M_U M_U^\dagger = \frac{v^2}{2}\begin{pmatrix} |a_1|^2\lambda^6 + c_1^2\lambda^{16} & a_1 a_2\lambda^5 & a_1 a_3\lambda^3 \\ a_1^* a_2\lambda^5 & a_2^2\lambda^4 + b_1^2\lambda^8 & a_2 a_3\lambda^2 \\ a_1^* a_3\lambda^3 & a_2 a_3\lambda^2 & a_3^2 \end{pmatrix}, \tag{12}$$

$$M_D M_D^T = \frac{v^2}{2}\begin{pmatrix} \lambda^{14}e_1^2 + \lambda^{12}f_1^2 & e_1e_2\lambda^{13} + f_1f_2\lambda^{11} & 0 \\ e_1e_2\lambda^{13} + f_1f_2\lambda^{11} & \lambda^{12}e_2^2 + \lambda^{10}f_2^2 & 0 \\ 0 & 0 & \lambda^6 g_1^2 \end{pmatrix}, \tag{13}$$

and are approximately diagonalized by unitary rotation matrices R_U and R_D:

$$R_U^\dagger M_U M_U^\dagger R_U = \begin{pmatrix} m_u^2 & 0 & 0 \\ 0 & m_c^2 & 0 \\ 0 & 0 & m_t^2 \end{pmatrix}, \qquad R_U \simeq \begin{pmatrix} c_{13} & s_{13}s_{23}e^{i\delta} & -c_{23}s_{13}e^{i\delta} \\ 0 & c_{23} & s_{23} \\ s_{13}e^{-i\delta} & -c_{13}s_{23} & c_{13}c_{23} \end{pmatrix}, \tag{14}$$

$$R_D^T M_D M_D^T R_D = \begin{pmatrix} m_d^2 & 0 & 0 \\ 0 & m_s^2 & 0 \\ 0 & 0 & m_b^2 \end{pmatrix}, \qquad R_D = \begin{pmatrix} c_{12} & s_{12} & 0 \\ -s_{12} & c_{12} & 0 \\ 0 & 0 & 1 \end{pmatrix}, \tag{15}$$

where $c_{ij} = \cos\theta_{ij}$, $s_{ij} = \sin\theta_{ij}$ (with $i \neq j$ and$i, j = 1, 2, 3$). θ_{ij} and δ are the quark mixing angles and the CP violating phase, respectively, in the usual parametrization. They are given by

$$\tan\theta_{12} \simeq \frac{f_1}{f_2}\lambda, \qquad \tan\theta_{23} \simeq \frac{a_2}{a_3}\lambda^2, \qquad \tan\theta_{13} \simeq \frac{|a_1|}{a_3}\lambda^3, \qquad \delta = -\arg(a_1). \tag{16}$$

Therefore, the up- and down-type quark masses are approximately given by

$$m_u \simeq c_1\lambda^8\frac{v}{\sqrt{2}}, \qquad m_c \simeq b_1\lambda^4\frac{v}{\sqrt{2}}, \qquad m_t \simeq a_3\frac{v}{\sqrt{2}}, \tag{17}$$

$$m_d \simeq |e_1 f_2 - e_2 f_1| \frac{\lambda^7}{\sqrt{2}} v, \qquad m_s \simeq f_2 \lambda^5 \frac{v}{\sqrt{2}}, \qquad m_b \simeq g_1 \lambda^3 \frac{v}{\sqrt{2}}. \tag{18}$$

We also find that the Cabbibo-Kobayashi-Maskawa (CKM) quark mixing matrix is approximately

$$V_{\mathrm{CKM}} = R_U^\dagger R_D \simeq \begin{pmatrix} c_{12}c_{13} & c_{13}s_{12} & e^{i\delta}s_{13} \\ e^{-i\delta}c_{12}s_{13}s_{23} - c_{23}s_{12} & c_{12}c_{23} + e^{-i\delta}s_{12}s_{13}s_{23} & -c_{13}s_{23} \\ -s_{12}s_{23} - e^{-i\delta}c_{12}c_{23}s_{13} & c_{12}s_{23} - e^{-i\delta}c_{23}s_{12}s_{13} & c_{13}c_{23} \end{pmatrix}. \tag{19}$$

It is noteworthy that Eq. (11) provides an elegant understanding of all SM fermion masses and mixing angles through their scalings by powers of the Wolfenstein parameter $\lambda = 0.225$ with $\mathcal{O}(1)$ coefficients.

The Wolfenstein parametrization [56] of the CKM matrix is

$$V_W \simeq \begin{pmatrix} 1 - \frac{\lambda^2}{2} & \lambda & A\lambda^3(\rho - i\eta) \\ -\lambda & 1 - \frac{\lambda^2}{2} & A\lambda^2 \\ A\lambda^3(1-\rho-i\eta) & -A\lambda^2 & 1 \end{pmatrix}, \tag{20}$$

with

$$\lambda = 0.22537 \pm 0.00061, \qquad A = 0.814^{+0.023}_{-0.024}, \tag{21}$$

$$\bar{\rho} = 0.117 \pm 0.021, \qquad \bar{\eta} = 0.353 \pm 0.013, \tag{22}$$

$$\bar{\rho} \simeq \rho\left(1 - \frac{\lambda^2}{2}\right), \qquad \bar{\eta} \simeq \eta\left(1 - \frac{\lambda^2}{2}\right). \tag{23}$$

From the comparison with (20), we find

$$a_3 \simeq 1, \qquad a_2 \simeq A \simeq 0.81,$$
$$a_1 \simeq -A\sqrt{\rho^2 + \eta^2} e^{i\delta} \simeq -0.3 e^{i\delta}, \tag{24}$$

$$\delta = 67^\circ, \quad b_1 \simeq \frac{m_c}{\lambda^4 m_t} \simeq 1.43, \quad c_1 \simeq \frac{m_u}{\lambda^8 m_t} \simeq 1.27. \tag{25}$$

Note that a_1 is required to be complex, as previously assumed, and its magnitude is a bit smaller than the remaining $\mathcal{O}(1)$ coefficients.

Since the charged fermion masses and quark mixing hierarchy arise from the $Z_3' \otimes Z_{14}$ symmetry breaking, and in order to have the right value of the Cabibbo mixing, we need $e_2 \approx f_2$. We fit the parameters e_1, f_1, f_2 and g_1 in Eq. (11) to reproduce the down-type quark masses and quark mixing parameters. As can be seen from the above formulas, the quark sector of our model contains ten effective free parameters, i.e., $|a_1|$, a_2, a_3, b_1, c_1, e_1, f_1, f_2, g_1 and the phase $\arg(a_1)$, to describe the quark mass and mixing pattern, which is characterized by ten physical observables, i.e., the six quark masses, the three mixing angles and the CP violating phase. Furthermore, in our model these parameters are of the same order of magnitude. The results for the down-type quark masses, the three quark mixing angles and the CP violating phase δ in Tables III and IV correspond to the best-fit values:

$$e_1 \simeq 0.84, \quad f_1 \simeq 0.4, \quad f_2 \simeq 0.57, \quad g_1 \simeq 1.42. \tag{26}$$

As pointed out in [55], the CKM matrix in our model is consistent with the experimental data. The agreement of our model with the experimental data is as good as in the models of Refs. [9,11,29,33,47,57,58] and better than, for example, those in Refs. [59–66]. The obtained and experimental values of the magnitudes of the CKM parameters, i.e., three quark mixing parameters and the CP violating phase δ, are shown in Table III. The experimental values of the CKM magnitudes and the Jarlskog invariant are taken from Ref. [67], whereas the experimental values of the quark masses, which are given at the M_Z scale, have been taken from Ref. [68].

B. Lepton masses and mixing

This S_3 flavor model obtains the viable quark textures proposed in [55] as shown in Sec. II A. We now proceed to analyze the lepton sector of the model. From the charged

TABLE III. Model and experimental values of the quark masses.

Observable	Model value	Experimental value
m_u (MeV)	1.47	$1.45^{+0.56}_{-0.45}$
m_c (MeV)	641	635 ± 86
m_t (GeV)	172.2	$172.1 \pm 0.6 \pm 0.9$
m_d (MeV)	3.00	$2.9^{+0.5}_{-0.4}$
m_s (MeV)	59.2	$57.7^{+16.8}_{-15.7}$
m_b (GeV)	2.82	$2.82^{+0.09}_{-0.04}$

TABLE IV. Model and experimental values of CKM parameters.

Observable	Model value	Experimental value
$\sin\theta_{12}$	0.2257	0.2254
$\sin\theta_{23}$	0.0412	0.0413
$\sin\theta_{13}$	0.00352	0.00350
δ	68°	68°

lepton Yukawa terms of Eq. (8) it follows that the charged lepton mass matrix takes the following form:

$$M_l = \frac{v}{\sqrt{2}}\begin{pmatrix} x_1\lambda^8 & 0 & 0 \\ 0 & y_1\lambda^5 & z_1\lambda^3 \\ 0 & y_2\lambda^5 & z_2\lambda^3 \end{pmatrix}, \tag{27}$$

where x_1, y_1, y_2, z_1, z_2, are $\mathcal{O}(1)$ parameters, assumed to be real, for simplicity.

Then, the charged lepton mass matrix satisfies the following relations:

$$M_l M_l^T = \frac{v^2}{2}\begin{pmatrix} x_1^2\lambda^{16} & 0 & 0 \\ 0 & z_1^2\lambda^6 + y_1^2\lambda^{10} & z_1 z_2\lambda^6 + y_1 y_2\lambda^{10} \\ 0 & z_1 z_2\lambda^6 + y_1 y_2\lambda^{10} & z_2^2\lambda^6 + y_2^2\lambda^{10} \end{pmatrix}, \tag{28}$$

$$M_l^T M_l = \frac{v^2}{2}\begin{pmatrix} x_1^2\lambda^{16} & 0 & 0 \\ 0 & (y_1^2 + y_2^2)\lambda^{10} & (y_1 z_1 + y_2 z_2)\lambda^8 \\ 0 & (y_1 z_1 + y_2 z_2)\lambda^8 & (z_1^2 + z_2^2)\lambda^6 \end{pmatrix}. \tag{29}$$

Therefore, the matrix $M_l M_l^T$ can be diagonalized by rotation matrix R_l according to

$$R_l^T M_l M_l^T R_l = \begin{pmatrix} m_e^2 & 0 & 0 \\ 0 & m_\mu^2 & 0 \\ 0 & 0 & m_\tau^2 \end{pmatrix},$$
$$R_l = \begin{pmatrix} 1 & 0 & 0 \\ 0 & \cos\theta_l & -\sin\theta_l \\ 0 & \sin\theta_l & \cos\theta_l \end{pmatrix},$$
$$\tan\theta_l \simeq -\frac{z_1}{z_2}. \tag{30}$$

The charged lepton masses are approximately given by

$$m_e = x_1\lambda^8\frac{v}{\sqrt{2}},$$
$$m_\mu \simeq \frac{|y_1 z_2 - y_2 z_1|}{\sqrt{z_1^2 + z_2^2}}\lambda^5\frac{v}{\sqrt{2}},$$
$$m_\tau \simeq \sqrt{z_1^2 + z_2^2}\lambda^3\frac{v}{\sqrt{2}}. \tag{31}$$

From the neutrino Yukawa terms it follows that the full 5×5 neutrino mass matrix is

$$M_\nu = \begin{pmatrix} 0_{3\times 3} & M_\nu^D \\ (M_\nu^D)^T & M_R \end{pmatrix}, \tag{32}$$

where

$$M_\nu^D = \begin{pmatrix} \lambda^3\varepsilon_{11}^{(\nu)}\frac{v_2}{\sqrt{2}} & \lambda^3\varepsilon_{12}^{(\nu)}\frac{v_2}{\sqrt{2}} \\ \varepsilon_{21}^{(\nu)}\frac{v_1}{\sqrt{2}} & \varepsilon_{22}^{(\nu)}\frac{v_3}{\sqrt{2}} \\ \varepsilon_{31}^{(\nu)}\frac{v_1}{\sqrt{2}} & \varepsilon_{33}^{(\nu)}\frac{v_3}{\sqrt{2}} \end{pmatrix} = \begin{pmatrix} A & F \\ B & E \\ C & D \end{pmatrix},$$
$$M_R = \begin{pmatrix} M_1 & \frac{1}{2}M_{12} \\ \frac{1}{2}M_{12} & M_2 \end{pmatrix}. \tag{33}$$

Since $(M_R)_{ii} \gg v$, the light neutrino mass matrix is generated through a type I seesaw mechanism and is given by

$$M_L = M_\nu^D M_R^{-1}(M_\nu^D)^T = \begin{pmatrix} A & F \\ B & E \\ C & D \end{pmatrix}\begin{pmatrix} -\frac{4M_2}{M_{12}^2 - 4M_1M_2} & \frac{2M_{12}}{M_{12}^2 - 4M_1M_2} \\ \frac{2M_{12}}{M_{12}^2 - 4M_1M_2} & -\frac{4M_1}{M_{12}^2 - 4M_1M_2} \end{pmatrix}\begin{pmatrix} A & B & C \\ F & E & D \end{pmatrix}$$
$$= \begin{pmatrix} -\frac{4(M_2A^2 - M_{12}AF + M_1F^2)}{M_{12}^2 - 4M_1M_2} & \frac{2(BFM_{12} - 2ABM_2 - 2FEM_1 + AEM_{12})}{M_{12}^2 - 4M_1M_2} & \frac{2(CFM_{12} - 2ACM_2 - 2FDM_1 + ADM_{12})}{M_{12}^2 - 4M_1M_2} \\ \frac{2(BFM_{12} - 2ABM_2 - 2FEM_1 + AEM_{12})}{M_{12}^2 - 4M_1M_2} & -\frac{4(M_2B^2 - M_{12}BE + M_1E^2)}{M_{12}^2 - 4M_1M_2} & \frac{2(BDM_{12} - 2BCM_2 + CEM_{12} - 2DEM_1)}{M_{12}^2 - 4M_1M_2} \\ \frac{2(CFM_{12} - 2ACM_2 - 2FDM_1 + ADM_{12})}{M_{12}^2 - 4M_1M_2} & \frac{2(BDM_{12} - 2BCM_2 + CEM_{12} - 2DEM_1)}{M_{12}^2 - 4M_1M_2} & -\frac{4(M_2C^2 - M_{12}CD + M_1D^2)}{M_{12}^2 - 4M_1M_2} \end{pmatrix}$$
$$= \begin{pmatrix} W^2 & WX\cos\varphi & WY\cos(\varphi - \varrho) \\ WX\cos\varphi & X^2 & XY\cos\varrho \\ WY\cos(\varphi - \varrho) & XY\cos\varrho & Y^2 \end{pmatrix}. \tag{34}$$

In order to demonstrate that these structures can be fit to the data, we set $\varphi = \varrho$ for simplicity, to obtain

$$M_L = \begin{pmatrix} W^2 & \kappa WX & WY \\ \kappa WX & X^2 & \kappa XY \\ WY & \kappa XY & Y^2 \end{pmatrix}, \qquad \kappa = \cos\varphi. \tag{35}$$

Assuming that the neutrino Yukawa couplings are real, we find that for the normal (NH) and inverted (IH) mass hierarchies, the light neutrino mass matrix is diagonalized by a rotation matrix R_ν, according to

$$R_\nu^T M_L R_\nu = \begin{pmatrix} 0 & 0 & 0 \\ 0 & m_{\nu_2} & 0 \\ 0 & 0 & m_{\nu_3} \end{pmatrix}, \qquad R_\nu = \begin{pmatrix} -\frac{Y}{\sqrt{W^2+Y^2}} & \frac{W}{\sqrt{W^2+Y^2}}\sin\theta_\nu & \frac{W}{\sqrt{W^2+Y^2}}\cos\theta_\nu \\ 0 & \cos\theta_\nu & -\sin\theta_\nu \\ \frac{W}{\sqrt{W^2+Y^2}} & \frac{Y}{\sqrt{W^2+Y^2}}\sin\theta_\nu & \frac{Y}{\sqrt{W^2+Y^2}}\cos\theta_\nu \end{pmatrix}, \quad \text{for NH} \tag{36}$$

$$\tan\theta_\nu = -\sqrt{\frac{m_3 - X^2}{X^2 - m_2}}, \qquad m_{\nu_1} = 0, \qquad m_{\nu_{2,3}} = \frac{W^2 + X^2 + Y^2}{2} \mp \frac{\sqrt{(W^2 - X^2 + Y^2)^2 - 4\kappa^2 X^2 (W^2 + Y^2)}}{2}.$$

$$R_\nu^T M_L R_\nu = \begin{pmatrix} m_{\nu_1} & 0 & 0 \\ 0 & m_{\nu_2} & 0 \\ 0 & 0 & 0 \end{pmatrix}, \qquad R_\nu = \begin{pmatrix} \frac{W}{\sqrt{W^2+Y^2}} & -\frac{Y}{\sqrt{W^2+Y^2}}\sin\theta_\nu & -\frac{Y}{\sqrt{W^2+Y^2}}\cos\theta_\nu \\ 0 & \cos\theta_\nu & -\sin\theta_\nu \\ \frac{Y}{\sqrt{W^2+Y^2}} & \frac{W}{\sqrt{W^2+Y^2}}\sin\theta_\nu & \frac{W}{\sqrt{W^2+Y^2}}\cos\theta_\nu \end{pmatrix}, \quad \text{for IH}$$

$$\tan\theta_\nu = -\sqrt{\frac{m_2 - X^2}{X^2 - m_1}}, \qquad m_{\nu_{1,2}} = \frac{W^2 + X^2 + Y^2}{2} \mp \frac{1}{2}\sqrt{(W^2 - X^2 + Y^2)^2 - 4\kappa^2 X^2 (W^2 + Y^2)}, \qquad m_{\nu_3} = 0. \tag{37}$$

The smallness of the active neutrinos' masses is a consequence of their scaling with the inverse of the large Majorana neutrino masses, as expected from the type I seesaw mechanism implemented in our model.

With the rotation matrices in the charged lepton sector R_l, Eq. (30), and the neutrino sector R_ν, Eqs. (36) and (37) for NH and IH, respectively, we obtain the PMNS mixing matrix

$$U = R_l^T R_\nu = \begin{cases} \begin{pmatrix} -\frac{Y}{\sqrt{W^2+Y^2}} & \frac{W}{\sqrt{W^2+Y^2}}\sin\theta_\nu & \frac{W}{\sqrt{W^2+Y^2}}\cos\theta_\nu \\ \frac{W}{\sqrt{W^2+Y^2}}\sin\theta_l & \cos\theta_l\cos\theta_\nu + \frac{Y}{\sqrt{W^2+Y^2}}\sin\theta_l\sin\theta_\nu & \frac{Y}{\sqrt{W^2+Y^2}}\cos\theta_\nu\sin\theta_l - \cos\theta_l\sin\theta_\nu \\ \frac{W}{\sqrt{W^2+Y^2}}\cos\theta_l & \frac{Y}{\sqrt{W^2+Y^2}}\cos\theta_l\sin\theta_\nu - \cos\theta_\nu\sin\theta_l & \sin\theta_l\sin\theta_\nu + \frac{Y}{\sqrt{W^2+Y^2}}\cos\theta_l\cos\theta_\nu \end{pmatrix} & \text{for NH,} \\ \begin{pmatrix} \frac{W}{\sqrt{W^2+Y^2}} & -\frac{Y}{\sqrt{W^2+Y^2}}\sin\theta_\nu & -\frac{Y}{\sqrt{W^2+Y^2}}\cos\theta_\nu \\ \frac{Y}{\sqrt{W^2+Y^2}}\sin\theta_l & \cos\theta_l\cos\theta_\nu + \frac{W}{\sqrt{W^2+Y^2}}\sin\theta_\nu\sin\theta_l & \frac{W}{\sqrt{X^2+Y^2}}\sin\theta_l\cos\theta_\nu - \cos\theta_l\sin\theta_\nu \\ \frac{Y}{\sqrt{W^2+Y^2}}\cos\theta_l & \frac{W}{\sqrt{W^2+Y^2}}\sin\theta_\nu\cos\theta_l - \cos\theta_\nu\sin\theta_l & \sin\theta_l\sin\theta_\nu + \frac{W}{\sqrt{W^2+Y^2}}\cos\theta_l\cos\theta_\nu \end{pmatrix} & \text{for IH.} \end{cases} \tag{38}$$

By comparing with the standard parametrization we derive the mixing angles for NH and IH:

$$\sin^2\theta_{12} = \frac{W^2\sin^2\theta_\nu}{Y^2 + (1-\cos^2\theta_\nu)W^2},$$
$$\sin^2\theta_{13} = \frac{W^2\cos^2\theta_\nu}{W^2 + Y^2},$$
$$\sin^2\theta_{23} = \frac{(\sqrt{W^2+Y^2}\sin\theta_\nu\cos\theta_l - Y\cos\theta_\nu\sin\theta_l)^2}{(1-\cos^2\theta_\nu)W^2 + Y^2},$$
$$\text{for NH} \tag{39}$$

$$\sin^2\theta_{12} = \frac{Y^2\sin^2\theta_\nu}{W^2 + (1-\cos^2\theta_\nu)Y^2}, \qquad \sin^2\theta_{13} = \frac{Y^2\cos^2\theta_\nu}{W^2 + Y^2},$$
$$\sin^2\theta_{23} = \frac{(\sqrt{W^2+Y^2}\sin\theta_\nu\cos\theta_l - W\cos\theta_\nu\sin\theta_l)^2}{(1-\cos^2\theta_\nu)Y^2 + W^2},$$
$$\text{for IH.} \tag{40}$$

We further simplify the analysis by considering

$$x_1 = y_2 = z_1, \tag{41}$$

so that the charged lepton masses will be determined by three dimensionless effective parameters, i.e., x_1, y_1 and z_2, whereas the neutrino mass squared splittings and neutrino mixing parameters will be controlled by four dimensionless effective parameters, i.e., κ, W, X and Y. Varying the parameters x_1, y_1, z_2, κ, W, X and Y, we fit the charged lepton masses, the neutrino mass squared splittings Δm^2_{21}, Δm^2_{31} (defined as $\Delta m^2_{ij} = m_i^2 - m_j^2$) and the leptonic mixing angles $\sin^2\theta_{12}$, $\sin^2\theta_{13}$ and $\sin^2\theta_{23}$ to their experimental values for NH and IH. Therefore the lepton sector of our model contains seven effective free parameters, i.e., x_1, y_1, z_2, κ, W, X and Y, and describes the lepton masses and mixing pattern, characterized by eight physical observables, i.e., the three charged lepton masses, the two neutrino mass squared splittings and the three leptonic mixing angles. The results shown in Table V correspond to the following best-fit values:

$$\begin{gathered}\kappa \simeq 0.45, \qquad W \simeq 0.13\ \mathrm{eV}^{\frac{1}{2}}, \\ X \simeq 0.11\ \mathrm{eV}^{\frac{1}{2}}, \qquad Y \simeq 0.18\ \mathrm{eV}^{\frac{1}{2}}, \\ x_1 \simeq 0.42, \qquad y_1 \simeq 1.39, \qquad z_2 \simeq 0.77, \quad \text{for NH,}\end{gathered} \tag{42}$$

$$\begin{gathered}\kappa \simeq 4.03\times 10^{-3}, \qquad W \simeq 0.18\ \mathrm{eV}^{\frac{1}{2}}, \\ X \simeq 0.22\ \mathrm{eV}^{\frac{1}{2}}, \qquad Y \simeq 0.13\ \mathrm{eV}^{\frac{1}{2}}, \\ x_1 \simeq 0.42, \qquad y_1 \simeq 1.38, \qquad z_2 \simeq 0.78, \quad \text{for IH.}\end{gathered} \tag{43}$$

Using the best-fit values given above, we obtain the following neutrino masses for NH and IH:

TABLE V. Model and experimental values of the lepton sector observables, for normal (NH) and inverted (IH) hierarchies.

Observable	Model value	Experimental value
m_e (MeV)	0.487	0.487
m_μ (MeV)	102.8	102.8 ± 0.0003
m_τ (GeV)	1.75	1.75 ± 0.0003
Δm^2_{21} (10^{-5} eV^2) (NH)	7.60	$7.60^{+0.19}_{-0.18}$
Δm^2_{31} (10^{-3} eV^2) (NH)	2.48	$2.48^{+0.05}_{-0.07}$
$\sin^2\theta_{12}$ (NH)	0.323	0.323 ± 0.016
$\sin^2\theta_{23}$ (NH)	0.567	$0.567^{+0.032}_{-0.128}$
$\sin^2\theta_{13}$ (NH)	0.0234	0.0234 ± 0.0020
Δm^2_{21} (10^{-5} eV^2) (IH)	7.60	$7.60^{+0.19}_{-0.18}$
Δm^2_{13} (10^{-3} eV^2) (IH)	2.48	$2.48^{+0.05}_{-0.06}$
$\sin^2\theta_{12}$ (IH)	0.323	0.323 ± 0.016
$\sin^2\theta_{23}$ (IH)	0.573	$0.573^{+0.025}_{-0.043}$
$\sin^2\theta_{13}$ (IH)	0.0240	0.0240 ± 0.0019

$$m_1 = 0, \quad m_2 \simeq 9\ \mathrm{meV}, \quad m_3 \simeq 50\ \mathrm{meV}, \quad \text{for NH,} \tag{44}$$

$$m_1 \simeq 49\ \mathrm{meV}, \quad m_2 \simeq 50\ \mathrm{meV}, \quad m_3 = 0, \quad \text{for IH.} \tag{45}$$

The obtained and experimental values of the observables in the lepton sector are shown in Table V. Given that the lightest neutrino is predicted to be massless in our model, the neutrino masses are hierarchical, which puts the overall neutrino mass scale below the current experimental reach (the same applies to the cosmological bound $\sum_{k=1}^3 m_{\nu_k} < 0.23$ eV on the sum of the neutrino masses [69,70]). Therefore, our model fulfills the cosmological contraints on neutrino masses for both normal and inverted hierarchies.

The experimental values of the charged lepton masses, which are given at the M_Z scale, have been taken from Ref. [68], whereas the experimental values of the neutrino mass squared splittings and leptonic mixing angles for both NH and IH are taken from Ref. [71]. The obtained charged lepton masses, neutrino mass squared splittings and lepton mixing angles are in excellent agreement with the experimental data, showing that the model can perfectly account for all the observables in the lepton sector. We recall that for the sake of simplicity, we assumed all leptonic parameters to be real and further restricted the set of parameters, but a nonvanishing CP violating phase in the PMNS mixing matrix can be generated by allowing one or several parameters in the neutrino mass matrix of Eq. (32) to be complex.

We can now predict the amplitude for neutrinoless double beta ($0\nu\beta\beta$) decay in our model, which is proportional to the effective Majorana neutrino mass

$$m_{\beta\beta} = \left|\sum_k U_{ek}^2 m_{\nu_k}\right|, \tag{46}$$

where U_{ek}^2 and m_{ν_k} are the PMNS mixing matrix elements and the Majorana neutrino masses, respectively.

Then, from Eqs. (38) and (42)–(45), we predict the following effective neutrino masses for both hierarchies:

$$m_{\beta\beta} = \begin{cases} 4\ \text{meV} & \text{for NH} \\ 50\ \text{meV} & \text{for IH} \end{cases}. \tag{47}$$

This is beyond the reach of the present and forthcoming $0\nu\beta\beta$-decay experiments. The present best upper limit on this parameter $m_{\beta\beta} \leq 160$ meV comes from the recently quoted EXO-200 experiment [72,73] $T_{1/2}^{0\nu\beta\beta}(^{136}\text{Xe}) \geq 1.6 \times 10^{25}$ yr at 90% C.L. This limit will be improved within the not-too-distant future. The GERDA experiment [74,75] is currently moving to phase II, at the end of which it is expected to reach $T_{1/2}^{0\nu\beta\beta}(^{76}\text{Ge}) \geq 2 \times 10^{26}$ yr, corresponding to $m_{\beta\beta} \leq 100$ MeV. A bolometric CUORE experiment, using ^{130}Te [76], is currently under construction. Its estimated sensitivity is around $T_{1/2}^{0\nu\beta\beta}(^{130}\text{Te}) \sim 10^{26}$ yr corresponding to $m_{\beta\beta} \leq 50$ meV. There are also proposals for ton-scale next-to-next generation $0\nu\beta\beta$ experiments with ^{136}Xe [77,78] and ^{76}Ge [74,79] claiming sensitivities over $T_{1/2}^{0\nu\beta\beta} \sim 10^{27}$ yr, corresponding to $m_{\beta\beta} \sim 12-30$ meV. For recent experimental reviews, see for example Ref. [80] and references therein. Thus, according to Eq. (47) our model predicts $T_{1/2}^{0\nu\beta\beta}$ at the level of sensitivities of the next generation or next-to-next generation $0\nu\beta\beta$ experiments.

III. SCALAR PHENOMENOLOGY

The renormalizable scalar potential involving only the $SU(2)$ doublets ϕ_i is

$$\begin{aligned} V(\phi_i) &= -\sum_{i=1}^{2}\mu_i^2(\phi_i^\dagger\phi_i) + \sum_{i=1}^{2}\kappa_i(\phi_i^\dagger\phi_i)^2, \\ V(\phi_1,\phi_2) &= \gamma_{12}(\phi_1^\dagger\phi_1)(\phi_2^\dagger\phi_2) + \kappa_{12}(\phi_1^\dagger\phi_2)(\phi_2^\dagger\phi_1), \\ V(\xi,\chi,\zeta,\phi_i) &= (\lambda_\xi(\xi\xi)_1 + \lambda_\chi(\chi^\dagger\chi) \\ &\quad + \lambda_\zeta(\zeta^\dagger\zeta))\sum_{i=1}^{2}\lambda_{1i}(\phi_i^\dagger\phi_i), \end{aligned}$$

whereas the remaining terms are

$$\begin{aligned} V(\xi) &= -\mu_\xi^2(\xi\xi)_1 + \gamma_{\xi,3}(\xi\xi)_2\xi \\ &\quad + \kappa_{\xi,1}(\xi\xi)_1(\xi\xi)_1 + \kappa_{\xi,2}(\xi\xi)_2(\xi\xi)_2, \\ V(\chi) &= -\mu_\chi^2(\chi^\dagger\chi) + \kappa_\chi(\chi^\dagger\chi)^2, \\ V(\zeta) &= -\mu_\zeta^2(\zeta^\dagger\zeta) + \kappa_\zeta(\zeta^\dagger\zeta)^2, \\ V(\xi,\chi,\zeta) &= \lambda_2(\xi\xi)_1(\chi^\dagger\chi) + \lambda_3(\xi\xi)_1(\zeta^\dagger\zeta) + \lambda_4(\zeta^\dagger\zeta)(\chi^\dagger\chi). \end{aligned}$$

To obtain a viable low-energy model with one CP-odd and one charged Goldstone boson, we consider the following soft breaking terms:

$$V_{\text{soft}}(\zeta,\chi) = -\mu_{\chi\zeta}^2(\zeta\chi + \zeta^\dagger\chi^\dagger), \tag{48}$$

$$V_{\text{soft}}(\phi_i,\phi_j) = -\mu_{12}^2[(\phi_1^\dagger\phi_2) + (\phi_2^\dagger\phi_1)]. \tag{49}$$

The mass matrices of the low-energy CP-even neutral scalars $\rho_{1,2}$; CP-odd neutral scalars $\eta_{1,2}$; and charged scalars $\varphi_{1,2}^\pm$ can be written as

$$\begin{aligned} M_1 &= \frac{1}{2}\begin{pmatrix} 2\kappa_1 v_1^2 + \frac{v_2}{v_1}\mu_{12}^2 & \gamma v_1 v_2 - \mu_{12}^2 \\ \gamma v_1 v_2 - \mu_{12}^2 & 2\kappa_2 v_2^2 + \frac{v_1}{v_2}\mu_{12}^2 \end{pmatrix}, \\ M_2 &= \frac{\mu_{12}^2}{2}\begin{pmatrix} \frac{v_2}{v_1} & -1 \\ -1 & \frac{v_1}{v_2} \end{pmatrix}, \\ M_3 &= \frac{\mu_{12}^2 + \kappa_{12}v_1 v_2}{2}\begin{pmatrix} \frac{v_2}{v_1} & -1 \\ -1 & \frac{v_1}{v_2} \end{pmatrix}. \end{aligned} \tag{50}$$

The physical low-energy scalar mass eigenstates are connected with the weak scalar states by the following relations [81,82],

$$\begin{aligned} \begin{pmatrix} h \\ H \end{pmatrix} &= \begin{pmatrix} \sin\alpha & -\cos\alpha \\ -\cos\alpha & -\sin\alpha \end{pmatrix}\begin{pmatrix} \rho_1 \\ \rho_2 \end{pmatrix}, \\ \tan 2\alpha &= \frac{2(\gamma v_1 v_2 - \mu_{12}^2)}{2(\kappa_1 v_1^2 - \kappa_2 v_2^2) + \mu_{12}^2(\frac{v_2}{v_1} - \frac{v_1}{v_2})}, \\ \begin{pmatrix} \pi^0 \\ A^0 \end{pmatrix} &= \begin{pmatrix} \cos\beta & \sin\beta \\ \sin\beta & -\cos\beta \end{pmatrix}\begin{pmatrix} \eta_1 \\ \eta_2 \end{pmatrix}, \\ \begin{pmatrix} \pi^\pm \\ H^\pm \end{pmatrix} &= \begin{pmatrix} \cos\beta & \sin\beta \\ \sin\beta & -\cos\beta \end{pmatrix}\begin{pmatrix} \varphi_1^\pm \\ \varphi_2^\pm \end{pmatrix}, \\ \tan\beta &= \frac{v_2}{v_1} \end{aligned} \tag{51}$$

with the low-energy physical scalar masses given by

$$m_h^2 = \frac{1}{2v_1}\left(\kappa_1 v_1^3 + \kappa_2 v_1 v_2^2 + \mu_{12}^2 v_2 - v_1\sqrt{\gamma^2 v_1^2 v_2^2 - 2\gamma\mu_{12}^2 v_1 v_2 + \kappa_1^2 v_1^4 - 2\kappa_1\kappa_2 v_1^2 v_2^2 + \kappa_2^2 v_2^4 + \mu_{12}^4}\right), \tag{52}$$

$$m_H^2 = \frac{1}{2v_1}\left(\kappa_1 v_1^3 + \kappa_2 v_1 v_2^2 + \mu_{12}^2 v_2 + v_1\sqrt{\gamma^2 v_1^2 v_2^2 - 2\gamma\mu_{12}^2 v_1 v_2 + \kappa_1^2 v_1^4 - 2\kappa_1\kappa_2 v_1^2 v_2^2 + \kappa_2^2 v_2^4 + \mu_{12}^4}\right), \tag{53}$$

$$m_{A^0}^2 = \frac{\mu_{12}^2}{2}\left(\frac{v_2}{v_1}+\frac{v_1}{v_2}\right),$$
$$m_{H^\pm}^2 = \frac{\mu_{12}^2+\kappa_{12}v_1v_2}{2}\left(\frac{v_2}{v_1}+\frac{v_1}{v_2}\right). \tag{54}$$

The physical low-energy scalar spectrum of our model includes two massive charged Higgs bosons ($H^\pm$), one CP-odd Higgs (A^0) and two neutral CP-even Higgs (h, H^0) bosons. The scalar h is identified as the SM-like 126 GeV Higgs boson found at the LHC. It it noteworthy that the neutral π^0 and charged $\pi^\pm$ Goldstone bosons are associated with the longitudinal components of the Z and $W^\pm$ gauge bosons, respectively.

Thanks to the specific shape of the Yukawa couplings dictated by the discrete symmetries, the present model is flavor conserving in the down-type and charged lepton sectors because for those sectors we have a special case of Yukawa alignment [83–85]. ϕ_2 generates the masses of the first two down-type quark generations, whereas ϕ_1 is responsible only for the bottom Yukawa; conversely, ϕ_2 is associated only with the electron Yukawa, while ϕ_1 generates the masses of the remaining charged leptons. The Yukawa couplings of both doublets are therefore aligned in these sectors. Due to the lack of flavor changing neutral currents (FCNCs) in the down-type sector, tightly constrained kaon and B-meson mixings are protected against neutral scalar contributions. Mixing occurs exclusively in the up-type sector, where both ϕ_1 and ϕ_2 couple to the third generation of up-type quarks. Consequently, top quark FCNCs arise that can be exploited as a probe of new physics since associated processes are strongly suppressed in the SM. Explicitly, we obtain the following structures for the up- and down-type Yukawas in the scalar and fermion mass bases using the rotation matrices (14), (30), (51) and the corresponding transformations of the right-handed fields:

$$Y_h^d = \begin{pmatrix} y_{dd}^h & y_{ds}^h & y_{db}^h \\ y_{sd}^h & y_{ss}^h & y_{sb}^h \\ y_{bd}^h & y_{bs}^h & y_{bb}^h \end{pmatrix} = \sqrt{2}\begin{pmatrix} -\frac{c_\alpha m_d}{v s_\beta} & 0 & 0 \\ 0 & -\frac{c_\alpha m_s}{v s_\beta} & 0 \\ 0 & 0 & \frac{m_b s_\alpha}{v c_\beta} \end{pmatrix}, \tag{55}$$

$$Y_H^d = \begin{pmatrix} y_{dd}^H & y_{ds}^H & y_{db}^H \\ y_{sd}^H & y_{ss}^H & y_{sb}^H \\ y_{bd}^H & y_{bs}^H & y_{bb}^H \end{pmatrix} = \sqrt{2}\begin{pmatrix} -\frac{m_d s_\alpha}{v s_\beta} & 0 & 0 \\ 0 & -\frac{m_s s_\alpha}{v s_\beta} & 0 \\ 0 & 0 & -\frac{c_\alpha m_b}{v c_\beta} \end{pmatrix}, \tag{56}$$

$$Y_h^u = \begin{pmatrix} y_{uu}^h & y_{uc}^h & y_{ut}^h \\ y_{cu}^h & y_{cc}^h & y_{ct}^h \\ y_{tu}^h & y_{tc}^h & y_{tt}^h \end{pmatrix} \simeq \sqrt{2}\begin{pmatrix} \frac{m_u s_\alpha}{v c_\beta} & 0 & \frac{m_t}{v}V_{tb}V_{ub}(\frac{c_\alpha}{s_\beta}+\frac{s_\alpha}{c_\beta}) \\ 0 & \frac{m_c s_\alpha}{v c_\beta} & \frac{m_t}{v}V_{tb}V_{cb}(\frac{c_\alpha}{s_\beta}+\frac{s_\alpha}{c_\beta}) \\ 0 & 0 & \frac{m_t}{v}(V_{tb}^2\frac{s_\alpha}{c_\beta}-\frac{c_\alpha}{s_\beta}\mathcal{O}(\lambda^4)) \end{pmatrix}, \tag{57}$$

$$Y_H^u = \begin{pmatrix} y_{uu}^H & y_{uc}^H & y_{ut}^H \\ y_{cu}^H & y_{cc}^H & y_{ct}^H \\ y_{tu}^H & y_{tc}^H & y_{tt}^H \end{pmatrix} \simeq \sqrt{2}\begin{pmatrix} -\frac{c_\alpha m_u}{v c_\beta} & 0 & \frac{m_t}{v}V_{tb}V_{ub}(\frac{s_\alpha}{s_\beta}-\frac{c_\alpha}{c_\beta}) \\ 0 & -\frac{c_\alpha m_c}{v c_\beta} & \frac{m_t}{v}V_{tb}V_{cb}(\frac{s_\alpha}{s_\beta}-\frac{c_\alpha}{c_\beta}) \\ 0 & 0 & -\frac{m_t}{v}(V_{tb}^2\frac{c_\alpha}{c_\beta}+\frac{s_\alpha}{s_\beta}\mathcal{O}(\lambda^4)) \end{pmatrix}, \tag{58}$$

with the notations $\sin(x)\equiv s_x$, $\cos(x)\equiv c_x$ and $\tan(x)\equiv t_x$ and V_{ij} denote the CKM matrix elements. Furthermore, the mixing angles α and β are defined in Eq. (51). As in other 2HDMs the couplings depend crucially on the parameters α and β, but should comply with the current bounds if $\tan\beta$ is neither unnaturally large nor small, in which cases deviations from the bottom and top Yukawa couplings with respect to the SM will become very large. This agrees with our previous statement that the fermion mass hierarchies and mixing are best explained by $\tan\beta$ values of $\mathcal{O}(1)$. As explained above, FCNCs are absent in the down-type quark sector since the matrices $Y_{h,H}^d$ do not have off-diagonal entries. The up-type Yukawa couplings $Y_{ut,ct}^{h,H}$, however, allow for the tree-level decays $t\to hq$ $(q=u,c)$, whose branching ratios are currently limited by ATLAS to $\mathrm{Br}(t\to hq)<0.79\%$ @ 95% C.L. [86] and by CMS to $\mathrm{Br}(t\to hq)<0.56\%$ @ 95% C.L. (observed limit) and $\mathrm{Br}(t\to hq)<0.65^{+0.29}_{-0.19}\%$ (expected limit) [87]. Since y_{ut} is negligibly small compared to y_{ct}, we consider only the stronger CMS constraint that can be interpreted as an upper bound on the off-diagonal top Yukawas to

$$\sqrt{|y_{ct}^h|^2+|y_{ct}^h|^2} = \frac{\sqrt{2}m_t}{v}\sqrt{\left|V_{tb}V_{cb}\left(\frac{s_\alpha}{c_\beta}+\frac{c_\alpha}{s_\beta}\right)\right|^2} < 0.14, \tag{59}$$

which translates to

$$\left|\frac{c_{\alpha-\beta}}{c_\beta s_\beta}\right| \lesssim 3.40. \tag{60}$$

The $t\to ch$ channel is particularly interesting since its branching ratio $\mathrm{Br}(t\to hc)_{\mathrm{SM}}\simeq 10^{-15}$ [86] is extremely

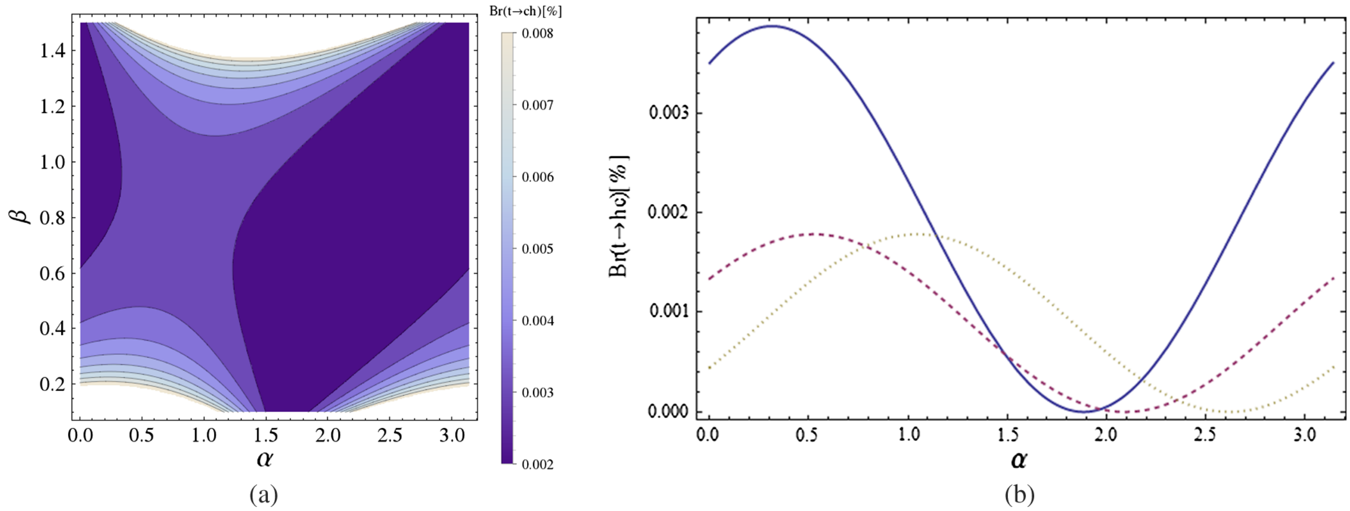

FIG. 1. (a) $\mathrm{Br}(t \to hc)[\%]$ in the $\alpha - \beta$ plane. (b) $\mathrm{Br}(t \to hc)[\%]$ as a function of α for $\beta = \pi/10$ (blue, solid), $\beta = \pi/6$ (red, dashed) and $\beta = \pi/3$ (yellow, dotted). The flavor violating $y_{ct}^{h,H}$ couplings are enhanced for small β values leading to a potentially large $\mathrm{Br}(t \to hc)$ observable at future experiments.

suppressed in the SM, but can be potentially large in our model, allowing it to be probed at future collider experiments. As shown in Fig. 1 our model predictions can reach branching ratios of $\mathcal{O}(0.01\%)$ in some regions of the $\alpha - \beta$ plane, allowing us to further constrain our model parameter space with experimental searches for rare top decays.

Recently an analysis of up-type FCNCs in the 2HDM type III has been performed [88], parametrizing the flavor violating y_{ct}^h coupling as $y_{ct}^h = \frac{1}{v}\lambda_{ct}\sqrt{2m_t m_c}$ according to the Cheng-Sher *ansatz* [89] (this type of FCNC was shown to be remarkably stable under radiative corrections [90]). Focusing on the $cc \to tt$ as well as the $t \to cg$ channels, they find that λ_{ct} can still take values of up to 10–20 depending on the neutral heavy Higgs mass. With $y_{ct}^h \propto \frac{1}{v} V_{cb} V_{tb} \sqrt{2} m_t$ our model corresponds to $\lambda_{ct} \approx \frac{1}{2}$ and is therefore well below the critical region. Indeed, following the analysis of [91] we find numerically that the loop induced decays $t \to cg$, $t \to c\gamma$ and $t \to cZ$ are several orders of magnitude below the current LHC sensitivity. Explicitly, varying the free model parameters α, β and the scalar masses m_H, m_A and $m_{H^\pm}$, we expect the branching ratios to be approximately

$$\begin{aligned} \mathrm{Br}(t \to cg) &\sim \mathcal{O}(10^{-9}), \\ \mathrm{Br}(t \to c\gamma) &\sim \mathcal{O}(10^{-12}), \\ \mathrm{Br}(t \to cZ) &\sim \mathcal{O}(10^{-13}), \end{aligned} \tag{61}$$

as opposed to the current upper limits from ATLAS and CMS [92,93],

$$\mathrm{Br}(t \to cg) < 1.6 \times 10^{-4}, \qquad \mathrm{Br}(t \to c\gamma, cZ) < 5 \times 10^{-4}. \tag{62}$$

The largest branching ratio of the three channels, $\mathrm{Br}(t \to cg)$, is shown in Fig. 2(a) as a function of α and β for fixed m_H and m_A, and in 2(b) for variable m_H and m_A with fixed α and β. As it turns out, the charged Higgs contribution is tiny and does not affect the prediction for any values of $m_{H^\pm}$.

In the charged lepton sector we obtain

$$\begin{aligned} Y_h^l &= \sqrt{2}\begin{pmatrix} y_{ee}^h & y_{e\mu}^h & y_{e\tau}^h \\ y_{\mu e}^h & y_{\mu\mu}^h & y_{\mu\tau}^h \\ y_{\tau e}^h & y_{\tau\mu}^h & y_{\tau\tau}^h \end{pmatrix} \\ &= \sqrt{2}\begin{pmatrix} -\frac{c_\alpha m_e}{v s_\beta} & 0 & 0 \\ 0 & \frac{m_\mu s_\alpha}{v c_\beta} & 0 \\ 0 & 0 & \frac{m_\tau s_\alpha}{v c_\beta} \end{pmatrix}, \end{aligned} \tag{63}$$

$$\begin{aligned} Y_H^l &= \sqrt{2}\begin{pmatrix} y_{ee}^H & y_{e\mu}^H & y_{e\tau}^H \\ y_{\mu e}^H & y_{\mu\mu}^H & y_{\mu\tau}^H \\ y_{\tau e}^H & y_{\tau\mu}^H & y_{\tau\tau}^H \end{pmatrix} \\ &= \sqrt{2}\begin{pmatrix} -\frac{m_e s_\alpha}{v s_\beta} & 0 & 0 \\ 0 & -\frac{c_\alpha m_\mu}{v c_\beta} & 0 \\ 0 & 0 & -\frac{c_\alpha m_\tau}{v c_\beta} \end{pmatrix}. \end{aligned} \tag{64}$$

The charged leptons are also free of FCNCs due to the lack of off-diagonal Yukawa couplings. Consequently, the recently reported anomaly in $h \to \mu\tau$ decays cannot be explained in our present model, even though it was possible to account for this in other multi-Higgs models with S_3 or other discrete symmetries [94–97].

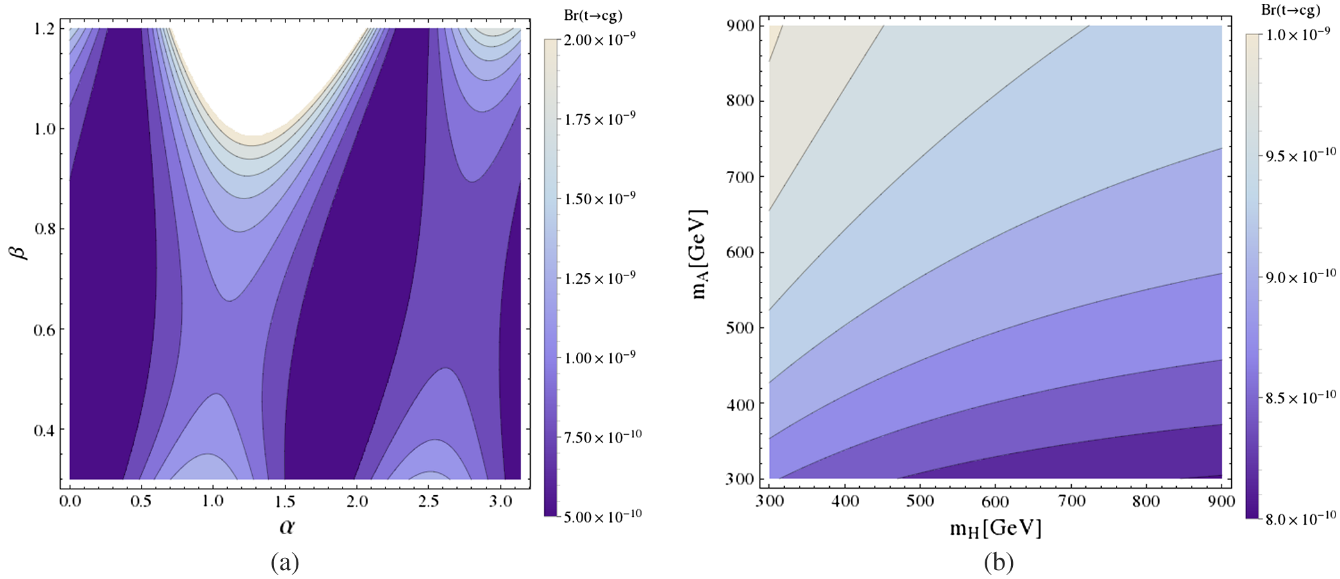

FIG. 2. (a) $\mathrm{Br}(t \to hg)$ in the $\alpha - \beta$ plane with $m_H = m_A = 500$ GeV. (b) $\mathrm{Br}(t \to hg)$ as a function of m_H and m_A for $\alpha = \pi/3$ and $\beta = \pi/4$. The decay rate is to a large extent independent of the charged Higgs mass $m_{H^\pm}$.

The charged Higgs couplings that are relevant, e.g., for $B^0_{s,d} - \overline{B^0}_{s,d}$ mixing and the radiative decays $b \to q\gamma$ $(q = s, d)$, are given by

$$Y^L_{H^\pm} = \sqrt{2}\begin{pmatrix} y_{du} & y_{dc} & y_{dt} \\ y_{su} & y_{sc} & y_{st} \\ y_{bu} & y_{bc} & y_{bt} \end{pmatrix} = \sqrt{2}\begin{pmatrix} \frac{V_{ud}}{V_{tb}^2+V_{cb}^2} t_\beta \frac{m_u}{v} & -\frac{V_{us}}{V_{tb}} t_\beta \frac{m_c}{v} & -V^*_{td}\frac{m_t}{v t_\beta} \\ \frac{V_{us}}{V_{tb}^2+V_{cb}^2} t_\beta \frac{m_u}{v} & \frac{V_{ud}}{V_{tb}} t_\beta \frac{m_c}{v} & -V^*_{ts}\frac{m_t}{v t_\beta} \\ 0 & 0 & V_{tb} t_\beta \frac{m_t}{v} \end{pmatrix}, \qquad (65)$$

$$Y^R_{H^\pm} = \sqrt{2}\begin{pmatrix} y_{ud} & y_{us} & y_{ub} \\ y_{cd} & y_{cs} & y_{cb} \\ y_{td} & y_{ts} & y_{tb} \end{pmatrix} = \sqrt{2}\begin{pmatrix} V_{ud}\frac{m_d}{v t_\beta} & V_{us}\frac{m_s}{v t_\beta} & V_{ub} t_\beta \frac{m_b}{v} \\ V_{cd}\frac{m_d}{v t_\beta} & V_{cs}\frac{m_s}{v t_\beta} & V_{cb} t_\beta \frac{m_b}{v} \\ V_{td}\frac{m_d}{v t_\beta} & V_{ts}\frac{m_s}{v t_\beta} & V_{tb} t_\beta \frac{m_b}{v} \end{pmatrix}, \qquad (66)$$

$$Y^{e\nu}_{H^\pm} = \sqrt{2}\frac{m_e}{v t_\beta}, \qquad Y^{\mu\nu}_{H^\pm} = \sqrt{2}\frac{m_\mu}{v} t_\beta (c_{\theta_l} - s_{\theta_l}),$$
$$Y^{\tau\nu}_{H^\pm} = \sqrt{2}\frac{m_\tau}{v} t_\beta (c_{\theta_l} + s_{\theta_l}), \qquad (67)$$

where in the last equation we summed over the neutrino mass eigenstates as they are usually undetected in typical flavor experiments. Here, the couplings y_{bu} and y_{bc} that could be used to explain the outstanding anomaly in $B \to D^{(*)}\tau\nu$ decays [98] are zero; hence no difference from 2HDMs of type II is to be expected in these channels.

On the other hand, the charged scalar sector is tightly constrained by $b \to s\gamma$ measurements, where the charged scalar $H^\pm$ leads to an additional loop diagram replacing the $W^\pm$. Recently a lower bound of 480 GeV was placed on the charged Higgs in the 2HDM type II [99]. Following the analysis of [100] we estimate a lower bound on the charged Higgs mass imposed on our model by constraints on the Wilson coefficients involved in $\mathrm{Br}(b \to s\gamma)$. Since $\tan\beta$ drops out in the product of the corresponding Yukawa couplings $y_{tb}(y_{bt})$ and $y_{ts}(y_{st})$, the prediction is independent of $\tan\beta$ and the lower limit is roughly $m_{H^\pm} \gtrsim 500$ GeV.

A. Constraints from $h \to \gamma\gamma$

In our 2HDM the $h \to \gamma\gamma$ decay receives additional contributions from loops with charged scalars $H^\pm$, as shown in Fig. 3, and therefore sets bounds on the masses of these scalars as well as on the angles α and β.

The explicit form of the $h \to \gamma\gamma$ decay rate is [101–108]

$$\Gamma(h \to \gamma\gamma) = \frac{\alpha_{em}^2 m_h^3}{256\pi^3 v^2}\Big|\sum\nolimits_f a_{hff} N_c Q_f^2 F_{1/2}(\varrho_f) + a_{hWW} F_1(\varrho_W) + \frac{\lambda_{hH^\pm H^\mp} v}{2 m^2_{H^\pm}} F_0(\varrho_{H^\pm})\Big|^2. \qquad (68)$$

Here ϱ_i are the mass ratios $\varrho_i = \frac{m_h^2}{4M_i^2}$, with $M_i = m_f, M_W$, and $m_{H^\pm}$; α_{em} is the fine structure constant; N_C is the color factor ($N_C = 1$ for leptons, $N_C = 3$ for quarks); and Q_f is the electric charge of the fermion in the loop. From the

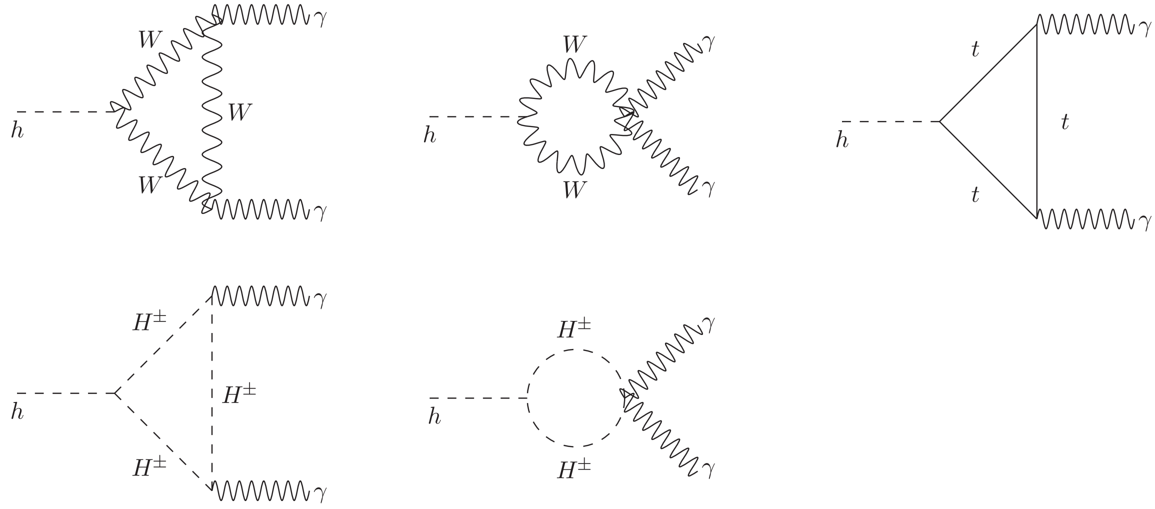

FIG. 3. One-loop Feynman diagrams in the unitary gauge contributing to the $h \to \gamma\gamma$ decay.

fermion-loop contributions we consider only the dominant top quark term. Furthermore, $\lambda_{hH^\pm H^\mp}$ is the trilinear coupling between the SM-like Higgs and a pair of charged Higgs bosons, which is given by

$$\lambda_{hH^\pm H^\mp} = -\frac{\gamma_{12} + \kappa_{12}}{2} v \sin 2\beta \cos(\alpha + \beta). \tag{69}$$

Besides that a_{htt} and a_{hWW} are the deviation factors from the SM Higgs–top quark coupling and the SM Higgs–W gauge boson coupling, respectively (in the SM these factors are unity). These deviation factors are given by

$$a_{htt} \simeq \frac{\sin\alpha}{\cos\beta}, \tag{70}$$

$$a_{hWW} = \sin(\alpha - \beta), \tag{71}$$

where in a_{htt} we neglected the contribution suppressed by small CKM entries.

The dimensionless loop factors $F_{1/2}(\varrho)$ and $F_1(\varrho)$ (for spin-$1/2$ and spin-1 particles in the loop, respectively) are [104,106]

$$F_{1/2}(\varrho) = 2[\varrho + (\varrho - 1)f(\varrho)]\varrho^{-2}, \tag{72}$$

$$F_1(\varrho) = -[2\varrho^2 + 3\varrho + 3(2\varrho - 1)f(\varrho)]\varrho^{-2}, \tag{73}$$

$$F_0(\varrho) = -[\varrho - f(\varrho)]\varrho^{-2}, \tag{74}$$

with

$$f(\varrho) = \begin{cases} \arcsin^2\sqrt{\varrho}, & \text{for } \varrho \leq 1 \\ -\frac{1}{4}\left[\ln\left(\frac{1+\sqrt{1-\varrho^{-1}}}{1-\sqrt{1-\varrho^{-1}}}\right) - i\pi\right]^2, & \text{for } \varrho \leq 1. \end{cases} \tag{75}$$

In what follows we determine the constraints that the Higgs diphoton signal strength imposes on our model. To this end, we introduce the ratio $R_{\gamma\gamma}$, which normalizes the $\gamma\gamma$ signal predicted by our model relative to that of the SM:

$$R_{\gamma\gamma} = \frac{\sigma(pp \to h)\Gamma(h \to \gamma\gamma)}{\sigma(pp \to h)_{\mathrm{SM}}\Gamma(h \to \gamma\gamma)_{\mathrm{SM}}} \simeq a_{htt}^2 \frac{\Gamma(h \to \gamma\gamma)}{\Gamma(h \to \gamma\gamma)_{\mathrm{SM}}}. \tag{76}$$

The normalization given by Eq. (76) for $h \to \gamma\gamma$ was also used in Refs. [94,108–113].

The ratio $R_{\gamma\gamma}$ has been measured by CMS and ATLAS with the best-fit signals [114,115]

$$R_{\gamma\gamma}^{\mathrm{CMS}} = 1.14^{+0.26}_{-0.23} \quad \text{and} \quad R_{\gamma\gamma}^{\mathrm{ATLAS}} = 1.17 \pm 0.27.$$

Figure 4(a) shows the sensitivity of the ratio $R_{\gamma\gamma}$ under variations of the mixing angle α for $m_{H^\pm} = 500$ GeV, $\gamma_{12} + \kappa_{12} = 1$ and different values of the mixing angle β. It follows that as the mixing angle β is increased, the range of α consistent with LHC observations of $h \to \gamma\gamma$ moves away from $\pi/2$. On the other hand, the decay rate is largely independent of the charged Higgs mass or the sum of the couplings $\gamma_{12} + \kappa_{12}$, which is consistent with the contribution mediated by charged scalars to the $h \to \gamma\gamma$ process being a small correction. In fact we checked numerically that it stays almost constant when $m_{H^\pm}$ is varied from 500 GeV to 1 TeV for fixed values of α, β, and the quartic couplings of the scalar potential. For the same values of the charged Higgs mass and quartic couplings, we show in Fig. 4(b) the Z-shaped allowed region in the $\alpha - \beta$ plane that is consistent with the Higgs diphoton decay rate constraints at the LHC, and overlay it with the relatively weak bound in Eq. (60) that arises from top quark FCNCs.

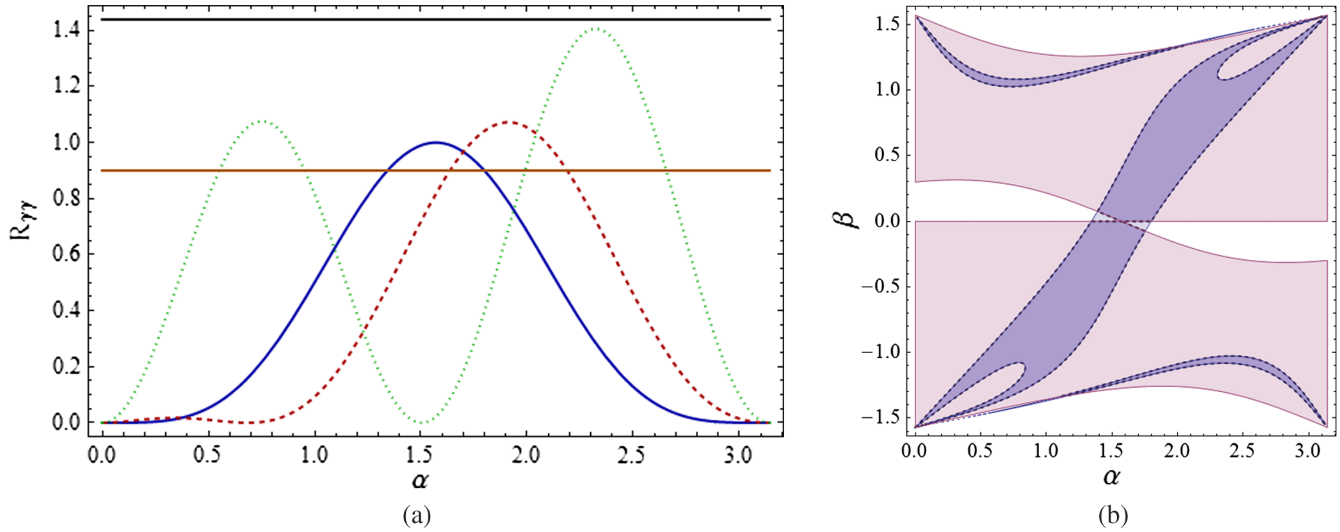

FIG. 4. The constraints on the model imposed by keeping $R_{\gamma\gamma}$ inside the experimentally allowed 1σ range determined by CMS and ATLAS to be $1.14^{+0.26}_{-0.23}$ and 1.17 ± 0.27, respectively [114,115]. (a) The ratio $R_{\gamma\gamma}$ as a function of the mixing angle α of the CP-even neutral scalars h and H^0 for $m_{H^\pm} = 500$ GeV, $\gamma_{12} + \kappa_{12} = 1$ and different values of the mixing angle β; the blue, red and green curves correspond to β set to 0, $\frac{\pi}{6}$ and $\frac{\pi}{3}$, respectively, and the horizontal lines are the minimum and maximum values of the ratio $R_{\gamma\gamma}$. (b) The allowed region in the $\alpha - \beta$ plane consistent with the Higgs diphoton decay rate constraint at the LHC, superimposed with the constraint imposed by Eq. (60).

B. T and S parameters

The extra scalars affect the oblique corrections of the SM, and these values are measured in high precision experiments. Consequently, they act as a further constraint on the validity of our model. The oblique corrections are parametrized in terms of the two well-known quantities T and S. In this section we calculate one-loop contributions to the oblique parameters T and S defined as [116–118]

$$T = \frac{\Pi_{33}(q^2) - \Pi_{11}(q^2)}{\alpha_{\rm EM}(M_Z)M_W^2}\bigg|_{q^2=0},$$
$$S = \frac{2\sin 2\theta_W}{\alpha_{\rm EM}(M_Z)}\frac{d\Pi_{30}(q^2)}{dq^2}\bigg|_{q^2=0}. \tag{77}$$

$\Pi_{11}(0)$, $\Pi_{33}(0)$, and $\Pi_{30}(q^2)$ are the vacuum polarization amplitudes with $\{W_\mu^1, W_\mu^1\}$, $\{W_\mu^3, W_\mu^3\}$ and $\{W_\mu^3, B_\mu\}$ external gauge bosons, respectively, where q is their momentum. We note that in the definitions of the T and S parameters, the new physics is assumed to be heavy when compared to M_W and M_Z.

The Feynman diagrams contributing to the T and S parameters are shown in Figs. 5 and 6.

We split the T and S, emphasizing the contributions arising from new physics as $T = T_{\rm SM} + \Delta T$ and $S = S_{\rm SM} + \Delta S$, where $T_{\rm SM}$ and $S_{\rm SM}$ are the SM contributions given by

$$T_{\rm SM} = -\frac{3}{16\pi\cos^2\theta_W}\ln\left(\frac{m_h^2}{m_W^2}\right), \tag{78}$$

$$S_{\rm SM} = \frac{1}{12\pi}\ln\left(\frac{m_h^2}{m_W^2}\right), \tag{79}$$

while ΔT and ΔS contain all the contributions involving in our model the heavy scalars

$$\begin{aligned}\Delta T \simeq &-\frac{3\cos^2(\alpha-\beta)}{16\pi\cos^2\theta_W}\ln\left(\frac{m_{H^0}^2}{m_h^2}\right)\\ &+\frac{1}{16\pi^2 v^2\alpha_{EM}(M_Z)}[m_{H^\pm}^2 - F(m_{A^0}^2, m_{H^\pm}^2)]\\ &+\frac{\sin^2(\alpha-\beta)}{16\pi^2 v^2\alpha_{\rm EM}(M_Z)}[F(m_h^2, m_{A^0}^2) - F(m_h^2, m_{H^\pm}^2)]\\ &+\frac{\cos^2(\alpha-\beta)}{16\pi^2 v^2\alpha_{\rm EM}(M_Z)}[F(m_{H^0}^2, m_{A^0}^2) - F(m_{H^0}^2, m_{H^\pm}^2)],\end{aligned} \tag{80}$$

$$\begin{aligned}\Delta S \simeq \frac{1}{12\pi}\bigg[&\cos^2(\alpha-\beta)\ln\left(\frac{m_{H^0}^2}{m_h^2}\right)\\ &+\sin^2(\alpha-\beta)K(m_h^2, m_{A^0}^2, m_{H^\pm}^2)\\ &+\cos^2(\alpha-\beta)K(m_{H^0}^2, m_{A^0}^2, m_{H^\pm}^2)\bigg],\end{aligned} \tag{81}$$

where we introduced the functions [104,119–125]

$$F(m_1^2, m_2^2) = \frac{m_1^2 m_2^2}{m_1^2 - m_2^2}\ln\left(\frac{m_1^2}{m_2^2}\right), \quad \lim_{m_2\to m_1} F(m_1^2, m_2^2) = m_1^2, \tag{82}$$

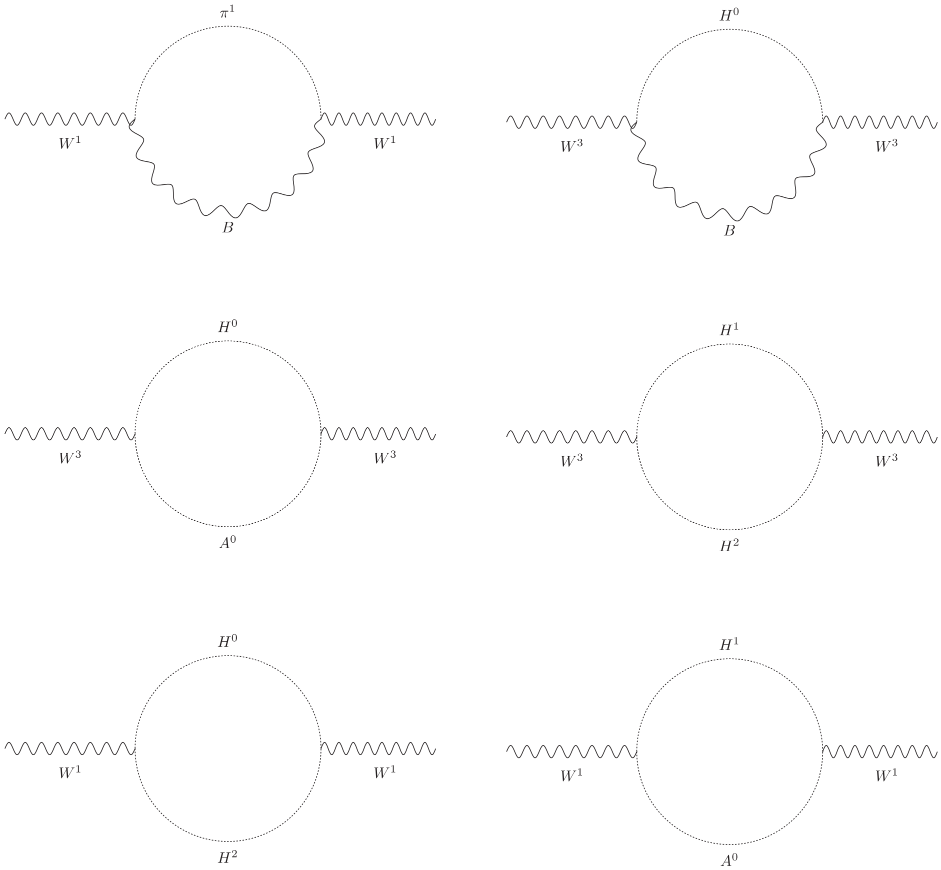

FIG. 5. One-loop Feynman diagrams contributing to the T parameter. The fields H^1 and H^2 are linear combinations of the charged Higgs bosons $H^{\pm}$, similarly to how $W^{\pm}$ gauge bosons are defined in terms of W^1 and W^2. Likewise, the fields π^1 and π^2 are linear combinations of the charged Goldstone bosons $\pi^{\pm}$.

$$K(m_1^2,m_2^2,m_3^2)=\frac{1}{(m_2^2-m_1^2)3}\left\{m_1^4(3m_2^2-m_1^2)\ln\left(\frac{m_1^2}{m_3^2}\right)-m_2^4(3m_1^2-m_2^2)\ln\left(\frac{m_2^2}{m_3^2}\right)-\frac{1}{6}[27m_1^2m_2^2(m_1^2-m_2^2)+5(m_2^6-m_1^6)]\right\}, \tag{83}$$

with the properties

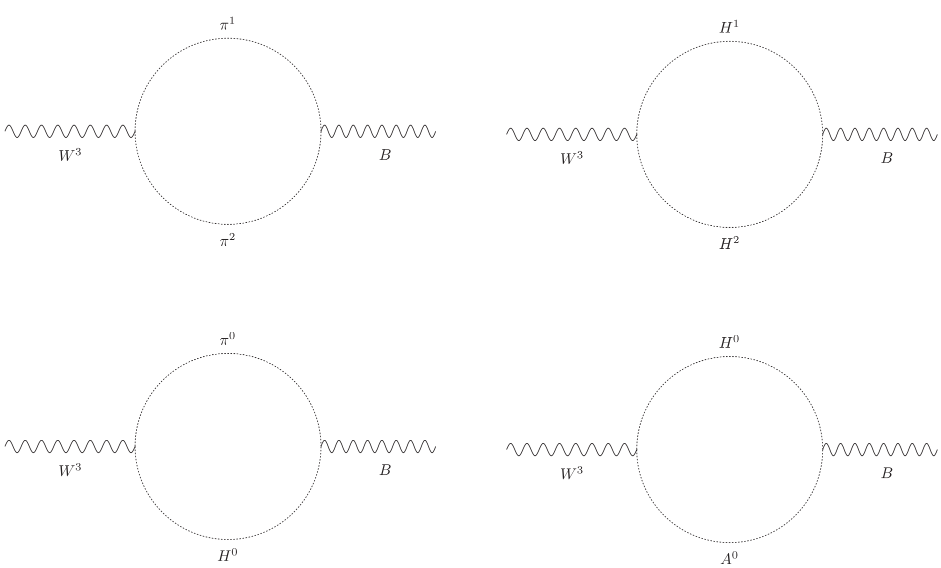

FIG. 6. One-loop Feynman diagrams contributing to the S parameter. The fields H^1 and H^2 are linear combinations of the charged Higgs bosons $H^{\pm}$, similarly to how $W^{\pm}$ gauge bosons are defined in terms of W^1 and W^2.

$$
\begin{aligned}
&\lim_{m_1\to m_2} K(m_1^2, m_2^2, m_3^2) = K_1(m_2^2, m_3^2) = \ln\left(\frac{m_2^2}{m_3^2}\right),\\
&\lim_{m_2\to m_3} K(m_1^2, m_2^2, m_3^2) = K_2(m_1^2, m_3^2) = \frac{-5m_1^6 + 27m_1^4 m_3^2 - 27m_1^2 m_3^4 + 6(m_1^6 - 3m_1^4 m_3^2)\ln(\frac{m_1^2}{m_3^2}) + 5m_3^6}{6(m_1^2 - m_3^2)^3},\\
&\lim_{m_1\to m_3} K(m_1^2, m_2^2, m_3^2) = K_2(m_2^2, m_3^2).
\end{aligned}
\tag{84}
$$

The experimental results on T and S restrict ΔT and ΔS to lie inside a region in the $\Delta S - \Delta T$ plane. At the 95% confidence level, these are the elliptic contours shown in Fig. 7. The origin $\Delta S = \Delta T = 0$ is the SM value with $m_h = 125.5$ GeV and $m_t = 176$ GeV. We analyze the T and S parameter constraints on our model by considering two benchmark scenarios, in both keeping $\alpha - \beta = \frac{\pi}{5}$. In the first scenario we assume that the CP-even and CP-odd neutral Higgs bosons have degenerate masses of 500 GeV, below which the LHC has not detected any scalars beyond the SM-like state. In this first scenario, we find that the T and S parameters constrain the charged Higgs masses to the range 550 GeV $\leq m_{H^\pm} \leq$ 580 GeV, which is consistent with the lower bound $m_{H^\pm} \gtrsim 500$ GeV obtained from $b \to s\gamma$ constraints [99]. In the second scenario, we assume that the charged Higgs bosons and CP-even neutral Higgs bosons have degenerate masses of 500 GeV. In this second scenario, the T and S parameter constraints are fulfilled if the CP-odd neutral Higgs boson mass is in the range 375 GeV $\leq m_{A^0} \leq$ 495 GeV.

IV. CONCLUSIONS

We have constructed a viable two-Higgs-doublet extension of the Standard Model which features additionally an S_3 flavor symmetry and extra scalars that break S_3. This leads to textures for fermion masses, and consists of an existence proof of models leading to the quark texture in [55]. Overall, the model can fit the observed masses and CKM and PMNS mixing angles very well. The model has in total seventeen effective free parameters, which are fitted to reproduce the experimental values of eighteen observables in the quark and lepton sectors, i.e., nine charged fermion masses, two neutrino mass squared splittings, three lepton mixing parameters, three quark mixing angles and one CP violating phase of the CKM quark mixing matrix. The model predicts

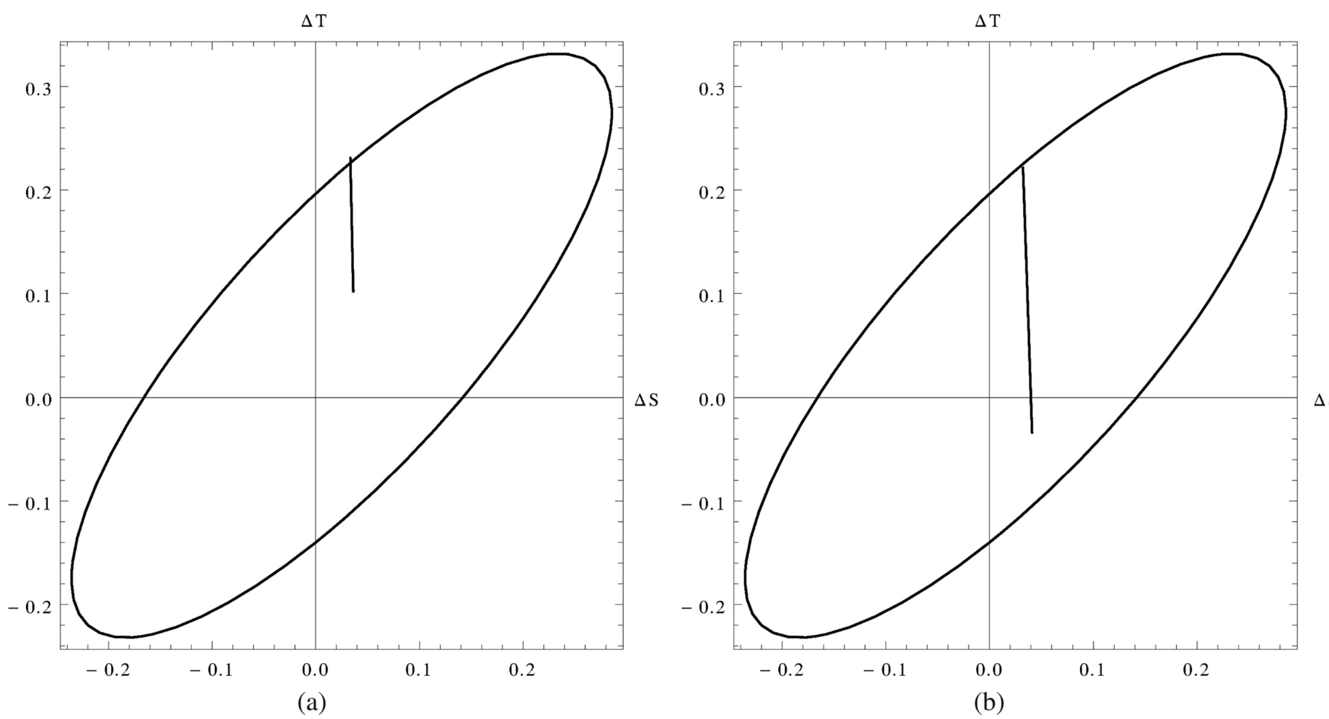

FIG. 7. The $\Delta S - \Delta T$ plane, where the ellipses contain the experimentally allowed region at 95% confidence level taken from [126–128]. We set $\alpha - \beta = \frac{\pi}{5}$. Figures (a) and (b) correspond to $m_{A^0} = m_{H^0} = 500$ GeV and $m_{H^0} = m_{H^\pm} = 500$ GeV, respectively. The charged Higgs and CP-odd neutral Higgs boson masses vary between (a) 550 GeV$\leq m_{H^\pm} \leq$ 580 GeV and (b) 375 GeV$\leq m_{A^0} \leq$ 495 GeV. The nearly vertical lines going up towards the ellipses correspond to ΔT and ΔS parameters in our model as masses are varied in the aforementioned ranges.

one massless neutrino for both normal and inverted hierarchies in the active neutrino mass spectrum as well as an effective Majorana neutrino mass, relevant for neutrinoless double beta decay, with values $m_{\beta\beta} = 4$ meV and 50 meV, for the normal and the inverted neutrino spectrum, respectively. In the latter case our prediction is within the declared reach of the next generation bolometric CUORE experiment [76] or, more realistically, of the next-to-next generation ton-scale $0\nu\beta\beta$-decay experiments. The sums of the light active neutrino masses in our model are 59 meV and 0.1 eV for the normal and the inverted neutrino spectra, respectively, which is consistent with the cosmological bound $\sum_{k=1}^{3} m_{\nu_k} < 0.23$ eV. The additional scalars mediate flavor changing neutral current processes, but due to the specific shape of the Yukawa couplings dictated by the flavor symmetry these processes occur only in the up-type quark sector. In the scalar sector the enlarged field content of the model leads to constraints from both rare top decays and from a $h \to \gamma\gamma$ rate that can be distinguished from the SM prediction. Among rare top decays, $t \to ch$ is particularly promising as its branching ratio can reach $\mathcal{O}(0.01\%)$ in our model. With respect to the $h \to \gamma\gamma$, we find that it depends only slightly on the mass of the charged Higgs and the dependence on the quartic scalar couplings is negligible, but the dominant top quark and vector boson contributions are modified in our model and allow us to place constraints on the hierarchy of the $SU(2)$ doublet VEVs (β) and the mixing of their CP-even mass eigenstates (α) that are much stronger than those obtained from the up-type quark flavor changing processes. We also showed for a few benchmark scenarios that our model is compatible with the present bounds for the oblique parameters T and S.

ACKNOWLEDGMENTS

This project has received funding from the European Union's Seventh Framework Programme for research, technological development and demonstration under Grant No. PIEF-GA-2012-327195 SIFT. A. E. C. H. thanks Southampton University for hospitality where part of this work was done. A. E. C. H. was supported by Fondecyt (Chile), Grant No. 11130115 and by DGIP internal Grant No. 111458.

APPENDIX A: THE PRODUCT RULES FOR S_3

The S_3 group has three irreducible representations: $\mathbf{1}$, $\mathbf{1'}$ and $\mathbf{2}$. Denoting the basis vectors for two S_3 doublets as $(x_1, x_2)^T$ and $(y_1, y_2)^T$ and y' a nontrivial S_3 singlet, the S_3 multiplication rules are [129]

$$\begin{pmatrix} x_1 \\ x_2 \end{pmatrix}_{\mathbf{2}} \otimes \begin{pmatrix} y_1 \\ y_2 \end{pmatrix}_{\mathbf{2}} = (x_1 y_1 + x_2 y_2)_{\mathbf{1}} + (x_1 y_2 - x_2 y_1)_{\mathbf{1'}} + \begin{pmatrix} x_2 y_2 - x_1 y_1 \\ x_1 y_2 + x_2 y_1 \end{pmatrix}_{\mathbf{2}}, \tag{A1}$$

$$\begin{pmatrix} x_1 \\ x_2 \end{pmatrix}_{\mathbf{2}} \otimes (y')_{\mathbf{1'}} = \begin{pmatrix} -x_2 y' \\ x_1 y' \end{pmatrix}_{\mathbf{2}}, \quad (x')_{\mathbf{1'}} \otimes (y')_{\mathbf{1'}} = (x' y')_{\mathbf{1}}. \tag{A2}$$

APPENDIX B: DECOUPLING AND S_3 VEVS

We assume that all SM singlet scalars acquire VEVs much larger than the electroweak symmetry breaking scale. This implies that the mixing angle between the scalar singlets and the $SU(2)$ doublet scalars is strongly suppressed since it is of the order of $\frac{v_{1,2}}{\lambda\Lambda}$, as it follows from the method of recursive expansion of Refs. [130–132]. Consequently, the mixing between these scalar singlets and the SM Higgs doublets can be neglected. We also checked numerically that the masses of the low-energy scalars are nearly unaffected by SM singlet VEVs of $\mathcal{O}(500\ \mathrm{GeV})$ and higher.

For simplicity we assume a CP invariant scalar potential with only real couplings as done in Refs. [10,11,42,94]. In the regime where the VEVs decouple, and also because the $1'$ scalar ζ is charged under Z_3', the relevant terms for determining the direction of the ξ VEV in S_3 are

$$V(\xi) = -\mu_\xi^2 (\xi\xi)_1 + \gamma_{\xi,3} (\xi\xi)_2 \xi + \kappa_{\xi,1} (\xi\xi)_1 (\xi\xi)_1 + \kappa_{\xi,2} (\xi\xi)_2 (\xi\xi)_2 + \kappa_{\xi,3} [(\xi\xi)_{\mathbf{2}} \xi]_{\mathbf{2}} \xi, \tag{B1}$$

From the minimization conditions of the high-energy scalar potential, we find the following relations:

$$\frac{\partial\langle V\rangle}{\partial v_{\xi_1}} = 2 v_{\xi_1} [\mu_\xi^2 + 2(\kappa_{\xi,1} + \kappa_{\xi,2} + \kappa_{\xi,3})(v_{\xi_1}^2 + v_{\xi_2}^2)] + 3\gamma_{\xi,3}(v_{\xi_2}^2 - v_{\xi_1}^2) = 0$$
$$\frac{\partial\langle V\rangle}{\partial v_{\xi_2}} = 2 v_{\xi_2} \{[\mu_\xi^2 + 2(\kappa_{\xi,1} + \kappa_{\xi,2} + \kappa_{\xi,3})(v_{\xi_1}^2 + v_{\xi_2}^2)] + 3\gamma_{\xi,3} v_{\xi_1}\} = 0. \tag{B2}$$

Then, from an analysis of the minimization equations given by Eq. (B2), we obtain for a large range of the parameter space the following VEV direction for ξ:

$$\langle\xi\rangle = v_\xi (1, 0). \tag{B3}$$

From the expressions given in Eq. (B2), and using the vacuum configuration for the S_3 scalar doublets given in Eq. (5), we find the relation between the parameters and the magnitude of the VEV:

$$\mu_\xi^2 = -\frac{v_\xi}{2} [3\gamma_{\xi,3} + 4(\kappa_{\xi,1} + \kappa_{\xi,2} + \kappa_{\xi,3}) v_\xi], \tag{B4}$$

These results show that the VEV direction for the S_3 doublet ξ in Eq. (5) is consistent with a global minimum of the scalar potential of our model.

[1] S. Pakvasa and H. Sugawara, Discrete symmetry and Cabibbo angle, Phys. Lett. B **73B**, 61 (1978).
[2] H. Cardenas, A. C. B. Machado, V. Pleitez, and J.-A. Rodriguez, Higgs decay rate to two photons in a model with two fermiophobic-Higgs doublets, Phys. Rev. D **87**, 035028 (2013).
[3] A. G. Dias, A. C. B. Machado, and C. C. Nishi, An S_3 model for lepton mass matrices with nearly minimal texture, Phys. Rev. D **86**, 093005 (2012).
[4] S. Dev, R. R. Gautam, and L. Singh, Broken S_3 symmetry in the neutrino mass matrix and non-zero θ_{13}, Phys. Lett. B **708**, 284 (2012).
[5] D. Meloni, S_3 as a flavour symmetry for quarks and leptons after the Daya Bay result on θ_{13}, J. High Energy Phys. 05 (2012) 124.
[6] F. González Canales, A. Mondragón, M. Mondragón, U. J. Saldaña Salazar, and L. Velasco-Sevilla, Quark sector of S3 models: Classification and comparison with experimental data, Phys. Rev. D **88**, 096004 (2013).
[7] E. Ma and B. Melic, Updated S_3 model of quarks, Phys. Lett. B **725**, 402 (2013).
[8] Y. Kajiyama, H. Okada, and K. Yagyu, Electron/muon specific two Higgs doublet model, Nucl. Phys. **B887**, 358 (2014).
[9] A. E. Cárcamo Hernández, R. Martínez, and F. Ochoa, Quark masses and mixing in $SU(3)_C \otimes SU(3)_L \otimes U(1)_X \otimes S_3$ models, arXiv:1309.6567.
[10] A. E. C. Hernández, E. C. Mur, and R. Martinez, Lepton masses and mixing in $SU(3)_C \otimes SU(3)_L \otimes U(1)_X$ models with a S_3 flavor symmetry, Phys. Rev. D **90**, 073001 (2014).
[11] A. E. C. Hernández, R. Martinez, and J. Nisperuza, S_3 discrete group as a source of the quark mass and mixing pattern in 331 models, Eur. Phys. J. C **75**, 72 (2015).
[12] V. V. Vien and H. N. Long, Neutrino mass and mixing in the 3-3-1 model and S_3 flavor symmetry with minimal Higgs content, Zh. Eksp. Teor. Fiz. **145**, 991 (2014) [J. Exp. Theor. Phys. **118**, 869 (2014)].
[13] E. Ma and R. Srivastava, Dirac or inverse seesaw neutrino masses with $B-L$ gauge symmetry and S_3 flavour symmetry, Phys. Lett. B **741**, 217 (2015).
[14] D. Das and U. K. Dey, Analysis of an extended scalar sector with S_3 symmetry, Phys. Rev. D **89**, 095025 (2014); **91**, 039905(E) (2015).
[15] D. Das, U. K. Dey, and P. B. Pal, S_3 symmetry and the CKM matrix, arXiv:1507.06509.
[16] E. Ma and G. Rajasekaran, Softly broken A(4) symmetry for nearly degenerate neutrino masses, Phys. Rev. D **64**, 113012 (2001).
[17] K. S. Babu, E. Ma, and J. W. F. Valle, Underlying A(4) symmetry for the neutrino mass matrix and the quark mixing matrix, Phys. Lett. B **552**, 207 (2003).
[18] G. Altarelli and F. Feruglio, Tri-bimaximal neutrino mixing from discrete symmetry in extra dimensions, Nucl. Phys. **B720**, 64 (2005).
[19] G. Altarelli and F. Feruglio, Tri-bimaximal neutrino mixing, A(4) and the modular symmetry, Nucl. Phys. **B741**, 215 (2006).
[20] I. de Medeiros Varzielas, S. F. King, and G. G. Ross, Tri-bimaximal neutrino mixing from discrete subgroups of SU(3) and SO(3) family symmetry, Phys. Lett. B **644**, 153 (2007).
[21] I. de Medeiros Varzielas and D. Pidt, UV completions of flavour models and large theta$_{13}$, J. High Energy Phys. 03 (2013) 065.
[22] H. Ishimori and E. Ma, New simple A_4 neutrino model for nonzero θ_{13} and large δ_{CP}, Phys. Rev. D **86**, 045030 (2012).
[23] Y. H. Ahn, S. K. Kang, and C. S. Kim, Spontaneous CP violation in A_4 flavor symmetry and leptogenesis, Phys. Rev. D **87**, 113012 (2013).
[24] N. Memenga, W. Rodejohann, and H. Zhang, A_4 flavor symmetry model for Dirac neutrinos and sizable U_{e3}, Phys. Rev. D **87**, 053021 (2013).
[25] S. Bhattacharya, E. Ma, A. Natale, and A. Rashed, Radiative scaling neutrino mass with A_4 symmetry, Phys. Rev. D **87**, 097301 (2013).
[26] P. M. Ferreira, L. Lavoura, and P. O. Ludl, A new A_4 model for lepton mixing, Phys. Lett. B **726**, 767 (2013).
[27] R. Gonzalez Felipe, H. Serodio, and J. P. Silva, Neutrino masses and mixing in A4 models with three Higgs doublets, Phys. Rev. D **88**, 015015 (2013).
[28] A. E. Carcamo Hernandez, I. de Medeiros Varzielas, S. G. Kovalenko, H. Päs, and I. Schmidt, Lepton masses and mixings in an A_4 multi-Higgs model with a radiative seesaw mechanism, Phys. Rev. D **88**, 076014 (2013).
[29] S. F. King, S. Morisi, E. Peinado, and J. W. F. Valle, Quark-lepton mass relation in a realistic A_4 extension of the Standard Model, Phys. Lett. B **724**, 68 (2013).
[30] S. Morisi, D. V. Forero, J. C. Romão, and J. W. F. Valle, Neutrino mixing with revamped A_4 flavor symmetry, Phys. Rev. D **88**, 036001 (2013).
[31] S. Morisi, M. Nebot, K. M. Patel, E. Peinado, and J. W. F. Valle, Quark-lepton mass relation and CKM mixing in an A4 extension of the minimal supersymmetric Standard Model, Phys. Rev. D **88**, 036001 (2013).
[32] R. González Felipe, H. Serôdio, and J. P. Silva, Models with three Higgs doublets in the triplet representations of A_4 or S_4, Phys. Rev. D **87**, 055010 (2013).
[33] M. D. Campos, A. E. Cárcamo Hernández, S. Kovalenko, I. Schmidt, and E. Schumacher, Fermion masses and mixings in an $SU(5)$ grand unified model with an extra flavor symmetry, Phys. Rev. D **90**, 016006 (2014).
[34] A. E. Cárcamo Hernández and R. Martinez, Lepton masses and mixings in a 331 model with A_4 flavour symmetry, arXiv:1501.05937.
[35] S. Pramanick and A. Raychaudhuri, An A4-based see-saw model for realistic neutrino mass and mixing, arXiv:1508.02330.
[36] C. Luhn, S. Nasri, and P. Ramond, Tri-bimaximal neutrino mixing and the family symmetry semidirect product of Z (7) and Z(3), Phys. Lett. B **652**, 27 (2007).
[37] C. Hagedorn, M. A. Schmidt, and A. Y. Smirnov, Lepton mixing and cancellation of the Dirac mass hierarchy in SO (10) GUTs with flavor symmetries T(7) and sigma(81), Phys. Rev. D **79**, 036002 (2009).
[38] Q. H. Cao, S. Khalil, E. Ma, and H. Okada, Observable T_7 Lepton Flavor Symmetry at the Large Hadron Collider, Phys. Rev. Lett. **106**, 131801 (2011).

[39] C. Luhn, K. M. Parattu, and A. Wingerter, A minimal model of neutrino flavor, J. High Energy Phys. 12 (2012) 096.
[40] Y. Kajiyama, H. Okada, and K. Yagyu, T_7 flavor model in three loop seesaw and Higgs phenomenology, J. High Energy Phys. 10 (2013) 196.
[41] C. Bonilla, S. Morisi, E. Peinado, and J. W. F. Valle, Relating quarks and leptons with the T_7 flavour group, Phys. Lett. B **742**, 99 (2015).
[42] A. E. C. Hernández and R. Martinez, Fermion mass and mixing pattern in a minimal T7 flavor 331 model, arXiv:1501.07261.
[43] C. Arbeláez, A. E. C. Hernández, S. Kovalenko, and I. Schmidt, Adjoint $SU(5)$ GUT model with T_7 flavor symmetry, arXiv:1507.03852.
[44] I. de Medeiros Varzielas, S. F. King, and G. G. Ross, Neutrino tri-bi-maximal mixing from a non-Abelian discrete family symmetry, Phys. Lett. B **648**, 201 (2007).
[45] E. Ma, Neutrino mass matrix from delta(27) symmetry, Mod. Phys. Lett. A **21**, 1917 (2006).
[46] I. de Medeiros Varzielas, D. Emmanuel-Costa, and P. Leser, Geometrical *CP* violation from non-renormalisable scalar potentials, Phys. Lett. B **716**, 193 (2012).
[47] G. Bhattacharyya, I. de Medeiros Varzielas, and P. Leser, A Common Origin of Fermion Mixing and Geometrical *CP* Violation, and Its Test through Higgs Physics at the LHC, Phys. Rev. Lett. **109**, 241603 (2012).
[48] E. Ma, Neutrino mixing and geometric *CP* violation with delta(27) symmetry, Phys. Lett. B **723**, 161 (2013).
[49] I. de Medeiros Varzielas and D. Pidt, Towards realistic models of quark masses with geometrical *CP* violation, J. Phys. G **41**, 025004 (2014).
[50] A. Aranda, C. Bonilla, S. Morisi, E. Peinado, and J. W. F. Valle, Dirac neutrinos from flavor symmetry, Phys. Rev. D **89**, 033001 (2014).
[51] I. de Medeiros Varzielas and D. Pidt, Geometrical *CP* violation with a complete fermion sector, J. High Energy Phys. 11 (2013) 206.
[52] I. de Medeiros Varzielas, $\Delta(27)$ family symmetry and neutrino mixing, J. High Energy Phys. 08 (2015) 157.
[53] S. F. King and C. Luhn, Neutrino mass and mixing with discrete symmetry, Rep. Prog. Phys. **76**, 056201 (2013).
[54] S. F. King, A. Merle, S. Morisi, Y. Shimizu, and M. Tanimoto, Neutrino mass and mixing: From theory to experiment, New J. Phys. **16**, 045018 (2014).
[55] A. E. C. Hernández and I. de Medeiros Varzielas, Viable textures for the fermion sector, J. Phys. G **42**, 065002 (2015).
[56] L. Wolfenstein, Parametrization of the Kobayashi-Maskawa Matrix, Phys. Rev. Lett. **51**, 1945 (1983).
[57] G. C. Branco, D. Emmanuel-Costa, and C. Simoes, Nearest-neighbour interaction from an Abelian symmetry and deviations from Hermiticity, Phys. Lett. B **690**, 62 (2010).
[58] A. E. Carcamo Hernandez and R. Rahman, Pseudo-Goldstone Higgs doublets from non-vectorlike grand unified Higgs sector, arXiv:1007.0447.
[59] M. C. Chen and K. T. Mahanthappa, CKM and Tri-bimaximal MNS Matrices in a $SU(5) \times^{(d)} T$ Model, Phys. Lett. B **652**, 34 (2007).
[60] Z. z. Xing, D. Yang, and S. Zhou, Broken S_3 flavor symmetry of leptons and quarks: Mass spectra and flavor mixing patterns, Phys. Lett. B **690**, 304 (2010).
[61] G. C. Branco, H. R. C. Ferreira, A. G. Hessler, and J. I. Silva-Marcos, Universality of strength of Yukawa couplings, quark singlets and strength of *CP* violation, J. High Energy Phys. 05 (2012) 001.
[62] A. E. Carcamo Hernandez, C. O. Dib, N. Neill, and A. R. Zerwekh, Quark masses and mixings in the RS1 model with a condensing 4th generation, J. High Energy Phys. 02 (2012) 132.
[63] V. V. Vien and H. N. Long, Quark masses and mixings in the 3-3-1 model with neutral leptons based on D_4 flavor symmetry, J. Korean Phys. Soc. **66**, 1809 (2015).
[64] M. Abbas and S. Khalil, Fermion masses and mixing in $\Delta(27)$ flavour model, Phys. Rev. D **91**, 053003 (2015).
[65] H. Ishimori and S. F. King, A model of quarks with $\Delta(6\mathrm{N}^2)$ family symmetry, Phys. Lett. B **735**, 33 (2014).
[66] H. Ishimori, S. F. King, H. Okada, and M. Tanimoto, Quark mixing from $\Delta(6\mathrm{N}^2)$ family symmetry, Phys. Lett. B **743**, 172 (2015).
[67] K. A. Olive *et al.* (Particle Data Group Collaboration), Review of particle physics, Chin. Phys. C **38**, 090001 (2014).
[68] K. Bora, Updated values of running quark and lepton masses at GUT scale in SM, 2HDM and MSSM, J. Phys. **2** (2013).
[69] P. A. R. Ade *et al.* (Planck Collaboration), Planck 2013 results. XVI. Cosmological parameters, Astron. Astrophys. **571**, A16 (2014).
[70] S. M. Bilenky, Neutrino in standard model and beyond, Phys. Part. Nucl. **46**, 475 (2015).
[71] D. V. Forero, M. Tortola, and J. W. F. Valle, Neutrino oscillations refitted, Phys. Rev. D **90**, 093006 (2014).
[72] M. Auger *et al.* (EXO-200 Collaboration), Search for Neutrinoless Double-Beta Decay in ^{136}Xe with EXO-200, Phys. Rev. Lett. **109**, 032505 (2012).
[73] D. J. Auty (EXO-200 Collaboration), Rencontres de Moriond, 2013, http://moriond.in2p3.fr/.
[74] I. Abt *et al.*, A new Ge^{76} double beta decay experiment at LNGS: Letter of intent, arXiv:hep-ex/0404039.
[75] K. H. Ackermann *et al.* (GERDA Collaboration), The GERDA experiment for the search of $0\nu\beta\beta$ decay in ^{76}Ge, Eur. Phys. J. C **73**, 2330 (2013).
[76] F. Alessandria *et al.*, Sensitivity of CUORE to neutrinoless double-beta decay, arXiv:1109.0494.
[77] A. Gando *et al.* (KamLAND-Zen Collaboration), Measurement of the double-β decay half-life of ^{136}Xe with the KamLAND-Zen experiment, Phys. Rev. C **85**, 045504 (2012).
[78] J. B. Albert *et al.* (EXO-200 Collaboration), Search for Majoron-emitting modes of double-beta decay of ^{136}Xe with EXO-200, Phys. Rev. D **90**, 092004 (2014).
[79] C. E. Aalseth *et al.* (Majorana Collaboration), The Majorana experiment, Nucl. Phys. B, Proc. Suppl. **217**, 44 (2011).
[80] S. M. Bilenky and C. Giunti, Neutrinoless double-beta decay: A probe of physics beyond the Standard Model, Int. J. Mod. Phys. A **30**, 1530001 (2015).

[81] G. C. Branco, P. M. Ferreira, L. Lavoura, M. N. Rebelo, M. Sher, and J. P. Silva, Theory and phenomenology of two-Higgs-doublet models, Phys. Rep. **516**, 1 (2012).
[82] G. Bhattacharyya and D. Das, Scalar sector of two-Higgs-doublet models: A mini-review, arXiv:1507.06424.
[83] A. Pich and P. Tuzon, Yukawa alignment in the two-Higgs-doublet model, Phys. Rev. D **80**, 091702 (2009).
[84] H. Serodio, Yukawa alignment in a multi Higgs doublet model: An effective approach, Phys. Lett. B **700**, 133 (2011).
[85] I. de Medeiros Varzielas, Family symmetries and alignment in multi-Higgs doublet models, Phys. Lett. B **701**, 597 (2011).
[86] G. Aad *et al.* (ATLAS Collaboration), Search for top quark decays $t \to qH$ with $H \to \gamma\gamma$ using the ATLAS detector, J. High Energy Phys. 06 (2014) 008.
[87] CMS Collaboration, Combined multilepton and diphoton limit on t to cH, Report No. CMS-PAS-HIG-13-034.
[88] C. S. Kim, Y. W. Yoon, and X. B. Yuan, Exploring top quark FCNC at hadron colliders in association with flavor physics, arXiv:1509.00491.
[89] T. P. Cheng and M. Sher, Mass matrix ansatz and flavor nonconservation in models with multiple Higgs doublets, Phys. Rev. D **35**, 3484 (1987).
[90] G. Cvetic, C. S. Kim, and S. S. Hwang, Higgs mediated flavor changing neutral currents in the general framework with two Higgs doublets: An RGE analysis, Phys. Rev. D **58**, 116003 (1998).
[91] D. Atwood, L. Reina, and A. Soni, Phenomenology of two Higgs doublet models with flavor changing neutral currents, Phys. Rev. D **55**, 3156 (1997).
[92] S. Chatrchyan *et al.* (CMS Collaboration), Search for Flavor-Changing Neutral Currents in Top-Quark Decays $t \to Zq$ in pp Collisions at $\sqrt{s} = 8$ TeV, Phys. Rev. Lett. **112**, 171802 (2014).
[93] G. Aad *et al.* (ATLAS Collaboration), Search for flavour-changing neutral current top-quark decays to qZ in pp collision data collected with the ATLAS detector at $\sqrt{s} = 8$ TeV, arXiv:1508.05796.
[94] M. D. Campos, A. E. C. Hernández, H. Päs, and E. Schumacher, Higgs $\to \mu\tau$ as an indication for S_4 flavor symmetry, Phys. Rev. D **91**, 116011 (2015).
[95] D. Aristizabal Sierra and A. Vicente, Explaining the CMS Higgs flavor violating decay excess, Phys. Rev. D **90**, 115004 (2014).
[96] J. Heeck, M. Holthausen, W. Rodejohann, and Y. Shimizu, Higgs ?t in Abelian and non-Abelian flavor symmetry models, Nucl. Phys. **B896**, 281 (2015).
[97] I. de Medeiros Varzielas, O. Fischer, and V. Maurer, $\mathbb{A}_4$ symmetry at colliders and in the universe, J. High Energy Phys. 08 (2015) 080.
[98] J. P. Lees *et al.* (*BABAR* Collaboration), Measurement of an excess of $\bar{B} \to D^{(*)}\tau^-\bar{\nu}_\tau$ decays and implications for charged Higgs bosons, Phys. Rev. D **88**, 072012 (2013).
[99] M. Misiak *et al.*, Updated NNLO QCD Predictions for the Weak Radiative B-Meson Decays, Phys. Rev. Lett. **114**, 221801 (2015).
[100] M. Trott and M. B. Wise, On theories of enhanced *CP* violation in $B_{s,d}$ meson mixing, J. High Energy Phys. 11 (2010) 157.
[101] M. A. Shifman, A. I. Vainshtein, M. B. Voloshin, and V. I. Zakharov, Low-energy theorems for Higgs boson couplings to photons, Yad. Fiz. **30**, 1368 (1979) [Sov. J. Nucl. Phys. **30**, 711 (1979)].
[102] M. B. Gavela, G. Girardi, C. Malleville, and P. Sorba, A nonlinear R(xi) gauge condition for the electroweak SU(2) X U(1) model, Nucl. Phys. **B193**, 257 (1981).
[103] P. Kalyniak, R. Bates, and J. N. Ng, Two photon decays of scalar and pseudoscalar bosons in supersymmetry, Phys. Rev. D **33**, 755 (1986).
[104] J. F. Gunion, H. E. Haber, G. L. Kane, and S. Dawson, The Higgs hunter's guide, Front. Phys. **80**, 1 (2000).
[105] M. Spira, QCD effects in Higgs physics, Fortschr. Phys. **46**, 203 (1998).
[106] A. Djouadi, The anatomy of electro-weak symmetry breaking. II. The Higgs bosons in the minimal supersymmetric model, Phys. Rep. **459**, 1 (2008).
[107] W. J. Marciano, C. Zhang, and S. Willenbrock, Higgs decay to two photons, Phys. Rev. D **85**, 013002 (2012).
[108] L. Wang and X. F. Han, The recent Higgs boson data and Higgs triplet model with vector-like quark, Phys. Rev. D **86**, 095007 (2012).
[109] A. E. Carcamo Hernandez, C. O. Dib, and A. R. Zerwekh, The effect of composite resonances on Higgs decay into two photons, Eur. Phys. J. C **74**, 2822 (2014).
[110] G. Bhattacharyya and D. Das, Nondecoupling of charged scalars in Higgs decay to two photons and symmetries of the scalar potential, Phys. Rev. D **91**, 015005 (2015).
[111] E. C. F. S. Fortes, A. C. B. Machado, J. Montaño, and V. Pleitez, Prediction of $h \to \gamma Z$ from $h \to \gamma\gamma$ at LHC for the IMDS_3 model, J. Phys. G **42**, 115001 (2015).
[112] A. E. Carcamo Hernandez, C. O. Dib, and A. R. Zerwekh, Composite resonances effects on EWPT and Higgs diphoton decay rate, arXiv:1503.08472.
[113] A. E. C. Hernández, C. O. Dib, and A. R. Zerwekh, Higgs boson coupling to a new strongly interacting sector, arXiv:1506.03631.
[114] V. Khachatryan *et al.* (CMS Collaboration), Observation of the diphoton decay of the Higgs boson and measurement of its properties, Eur. Phys. J. C **74**, 3076 (2014).
[115] G. Aad *et al.* (ATLAS Collaboration), Measurement of Higgs boson production in the diphoton decay channel in pp collisions at center-of-mass energies of 7 and 8 TeV with the ATLAS detector, Phys. Rev. D **90**, 112015 (2014).
[116] M. E. Peskin and T. Takeuchi, Estimation of oblique electroweak corrections, Phys. Rev. D **46**, 381 (1992).
[117] G. Altarelli and R. Barbieri, Vacuum polarization effects of new physics on electroweak processes, Phys. Lett. B **253**, 161 (1991).
[118] R. Barbieri, A. Pomarol, R. Rattazzi, and A. Strumia, Electroweak symmetry breaking after LEP-1 and LEP-2, Nucl. Phys. **B703**, 127 (2004).
[119] S. Bertolini, Quantum effects in a two Higgs doublet model of the electroweak interactions, Nucl. Phys. **B272**, 77 (1986).
[120] W. Hollik, Nonstandard Higgs bosons in SU(2) X U(1) radiative corrections, Z. Phys. C **32**, 291 (1986).
[121] W. Hollik, Radiative corrections with two Higgs doublets at LEP/SLC and HERA, Z. Phys. C **37**, 569 (1988).

[122] C. D. Froggatt, R. G. Moorhouse, and I. G. Knowles, Leading radiative corrections in two scalar doublet models, Phys. Rev. D **45**, 2471 (1992).

[123] W. Grimus, L. Lavoura, O. M. Ogreid, and P. Osland, The oblique parameters in multi-Higgs-doublet models, Nucl. Phys. **B801**, 81 (2008).

[124] H. E. Haber and D. O'Neil, Basis-independent methods for the two-Higgs-doublet model III: The *CP*-conserving limit, custodial symmetry, and the oblique parameters S, T, U, Phys. Rev. D **83**, 055017 (2011).

[125] A. E. Cárcamo Hernández, S. Kovalenko, and I. Schmidt, Precision measurements constraints on the number of Higgs doublets, Phys. Rev. D **91**, 095014 (2015).

[126] M. Baak and R. Kogler, The global electroweak Standard Model fit after the Higgs discovery, arXiv:1306.0571.

[127] M. Baak, M. Goebel, J. Haller, A. Hoecker, D. Kennedy, R. Kogler, K. Mönig, M. Schott, and J. Stelzer, The electroweak fit of the Standard Model after the discovery of a new boson at the LHC, Eur. Phys. J. C **72**, 2205 (2012).

[128] M. Baak, M. Goebel, J. Haller, A. Hoecker, D. Ludwig, K. Moenig, M. Schott, and J. Stelzer, Updated status of the global electroweak fit and constraints on new physics, Eur. Phys. J. C **72**, 2003 (2012).

[129] H. Ishimori, T. Kobayashi, H. Ohki, Y. Shimizu, H. Okada, and M. Tanimoto, Non-Abelian discrete symmetries in particle physics, Prog. Theor. Phys. Suppl. **183**, 1 (2010).

[130] W. Grimus and L. Lavoura, The seesaw mechanism at arbitrary order: Disentangling the small scale from the large scale, J. High Energy Phys. 11 (2000) 042.

[131] C. Alvarado, R. Martinez, and F. Ochoa, Quark mass hierarchy in 3-3-1 models, Phys. Rev. D **86**, 025027 (2012).

[132] A. E. Carcamo Hernandez, R. Martinez, and F. Ochoa, Radiative seesaw-type mechanism of quark masses in $SU(3)_C \otimes SU(3)_L \otimes U(1)_X$, Phys. Rev. D **87**, 075009 (2013).